International Journal of Earth Sciences
https://doi.org/10.1007/s00531-020-01914-9

ORIGINAL PAPER

Provenance analysis of Devonian peripheral foreland basins in SW Gondwana, case of the Gualilán Group, Precordillera Argentina

Jonatan Ariel Arnol[1] · Norberto Javier Uriz[2] · Carlos Alberto Cingolani[1,2] · Miguel Angelo Stipp Basei[3] · Paulina Abre[4]

Received: 24 October 2019 / Accepted: 15 July 2020

Abstract

We carried out a sedimentary provenance analysis of the Devonian Gualilán Group, Central Precordillera of western Argentina, focusing on the siliciclastic record of the Talacasto (Lower Devonian) and the Punta Negra (Lower-Middle Devonian) formations. Provenance is determined based on petrography, heavy minerals, whole-rock geochemistry, Sm–Nd isotopes, and U–Pb detrital zircon dating. Sandstones are composed of quartz, feldspar, and metamorphic and plutonic lithoclasts. The Gualilán Group underwent moderate weathering indicated by CIA values and Th/U ratios below 76 and 4.9, respectively. Th/Sc, Zr/Sc, Cr/V and La/Th ratios, negative Eu-anomalies and REE patterns point to felsic source compositions. The heavy minerals and zircon morphologies indicate that high-grade metamorphic and igneous rocks provided the bulk of detritus. T_{DM} ages between 1.40 and 1.46 Ga and $\varepsilon_{Nd(t)}$ values ranging from − 9.21 to − 11.13 constrain the signature of the sources. U–Pb detrital zircon ages for the Talacasto Formation are equally distributed between the Famatinian (Late Cambrian–Late Devonian), Pampean–Brazilian (Neoproterozoic–Early Cambrian) and Grenvillian-Sunsas (Mesoproterozoic) orogenic cycles. Detrital zircon ages of the Punta Negra Formation were dominantly supplied from Mesoproterozoic rocks, linked to the Grenvillian-Sunsas orogeny. The data indicate a provenance from rocks located eastwards of the basin represented by the basement of the Pampean Ranges. The peripheral foreland basin developed during the post-collisional regime that followed the accretion of Cuyania against Gondwana. Whereas eastern and western Pampean Ranges provided detritus to the Talacasto Formation, the Punta Negra Formation was sourced by the western Pampean Ranges, implying exhumation and erosion of such basement during the Devonian.

Keywords Provenance · Devonian Gualilán Group · Detrital zircon ages · Precordillera · SW Gondwana

Electronic supplementary material The online version of this article (https://doi.org/10.1007/s00531-020-01914-9) contains supplementary material, which is available to authorized users.

✉ Norberto Javier Uriz
norjuz@gmail.com

Jonatan Ariel Arnol
arnoljonatan@gmail.com

Carlos Alberto Cingolani
carloscingolani@yahoo.com

Miguel Angelo Stipp Basei
baseimas@usp.br

Paulina Abre
paulinabre@yahoo.com.ar

1 CIG (UNLP-CONICET) Centro de Investigaciones Geológicas, Facultad de Ciencias Naturales y Museo, Universidad Nacional de La Plata, Diag 113 N° 275, La Plata, Argentina

2 División Científica de Geología-Facultad de Ciencias Naturales y Museo, Universidad Nacional de La Plata (UNLP), Paseo del Bosque s/n, 1900, La Plata, Argentina

3 Instituto de Geociencias, Centro de Pesquisas Geocronológicas (CPGeo), Universidade de São Paulo, São Paulo, Brazil

4 Geología y Recursos Minerales, Centro Universitario Regional Este, Universidad de la República, Ruta 8, Treinta y Tres, Uruguay

Published online: 02 September 2020

Introduction

Eastward of the present-day Andes lies the Laurentian derived Cuyania terrane (Ramos et al. 1986; Ramos 2004), which is a constituent of the SW margin of Gondwana (Fig. 1) since the Late Cambrian–Late Devonian Famatinian orogenic cycle (Rapela et al. 1992, 1998; Ramos 1999). The Precordillera thin (and partially thick) skinned fold and thrust belt generated by Tertiary shallow east-dipping flat-slab subduction of the Nazca plate expose part of the sedimentary cover of the Cuyania terrane. It encompasses a 500 km north–south elongated belt with a maximum width of 110 km (from 28°30′ to 33° S and 68°15′ to 69°45′ W), along the provinces of La Rioja, San Juan and Mendoza of western Argentina (Fig. 1). The Cuyania terrane is stratigraphically and faunally unique to South America mainly for the Lower Paleozoic carbonate and siliciclastic successions overlying an unexposed igneous-metamorphic continental crust of Mesoproterozoic age (Ramos et al. 1998). In attempts to constrain its allochthonous or para-autochthonous origin with respect to Gondwana, researchers from several standpoints studied it during the last decades (Dalla Salda et al. 1992; Aceñolaza et al. 2002; Finney et al. 2003; Thomas and Astini 2003; and references therein). An array of geological and biostratigraphical evidence constrain the time of docking of the Cuyania terrane to the Middle Ordovician (Ramos 2004 and references therein). Subsequently, and until the Early-Middle Devonian, a time of certain tectonic stability linked to post-collisional regime allowed the development of important peripheral foreland basins.

The Cuyania terrane is bounded to the west by the Chilenia suspect terrane and, although its origin is still a matter of debate, its existence is supported by the occurrence of ophiolitic belts and P-T-t constraints indicating a collisional event at ca. 390 Ma, recorded in the Guarguaraz Complex (Willner et al. 2011; Massonne and Calderón 2008).

During the Devonian, the westward subduction of the Gondwana margin below the Chilenia terrain triggered the formation of an incipient magmatic arc with the development of small spaced plutons in the eastern margin of Chilenia, including, among others, the Pampa de los Avestruces granodiorite, La Menta and Borboran granites (375–390 Ma) in the Frontal Cordillera at approximately 36° S, (Davis et al. 1999; Tickyj et al. 2015; Cingolani and Ramos 2017 and references; Heredia et al. 2018). The brief subduction process closed the Chanic ocean developed between both continents. The collision and accretion of the Chilenia terrane against the proto-Andean margin of Gondwana during the Late Devonian, deformed the Silurian–Devonian sedimentary rocks, event also known as the Chanic tectonic phase (Ramos et al. 1986; Ramos 1999; Davis et al. 1999; Willner et al. 2011; Heredia et al. 2012; 2018; Cingolani and Ramos 2017). Devonian detrital zircon grains are not recorded in the rocks analysed for this work, probably due to the poor development of the arc, but they are found in the sedimentary rocks deposited in the active margin of southern Chilenia, overruling a subduction towards east proposed by Willner et al. (2011).

Fig. 1 **a** Regional location of the study area in South America. **b** Extension of the Precordillera as part of Cuyania terrane. Green square and yellow circle denote outcrops of the Villavicencio and Río Seco de los Castaños formations, respectively. **c** Tectonic subdivisions of the Precordillera. Eastern Precordillera is distinguished by Cambrian–Ordovician carbonate rocks; Central Precordillera shows a predominance of Ordovician carbonate rocks and Silurian–Devonian siliciclastic rocks, and Western Precordillera is characterized by Ordovician siliciclastic rocks. I–IV: studied sections in this work [modified from Ortiz and Zambrano (1981); Astini (1992); Ragona et al. (1995)]

In this tectonic setting, peripheral foreland basins developed in the western margin of the Cuyania terrane during the Devonian. An outstanding depocenter at the Central Precordillera of San Juan province preserves a siliciclastic record known as the Gualilán Group (Baldis 1975), comprising from base to top the Talacasto and Punta Negra formations (Cuerda and Baldis 1971; González Bonorino 1975; González Bonorino and Middleton 1976; Mingramm 1985; Astini 1991a; Peralta 1991; Bustos 1995, 1996; Bustos and Astini 1997; Herrera and Bustos 2001; Basilici et al. 2012; Vieira de Luca and Basilici 2013; Sterren et al. 2015). Deposition within a context of an extensional regime during the Devonian (Peralta 2005a, b, 2013; Peralta et al. 2008, 2010), is not supported by our data. Loske (1992, 1994 and 1995) acquired the first U–Pb detrital zircon ages of the Gualilán Group using the isotope dilution method and already linked main records to a Mesoproterozoic source exposed along the Pie de Palo Range (Fig. 1). This paper focuses on sedimentological features, mineralogical composition, lithogeochemistry, and U–Pb detrital zircon dating of the Gualilán Group to unravel its provenance. We assess the tectonic setting of the Devonian peripheral foreland basin in the context of the paleogeography of the SW Gondwana margin. Comparison to other Silurian–Devonian successions within the Cuyania terrane (i.e., Villavicencio and Río Seco de los Castaños formations) is also achieved, to constrain the paleogeographical evolution of depocentres.

Geological setting and stratigraphy

The Gualilán Group constitutes the principal Devonian succession of the Central Precordillera (Ortiz and Zambrano 1981) which integrates part of the so-called Eastern tectofacies (Astini 1992) of San Juan Province, Argentina. Its outcrops extend mainly throughout north–south ranges such as Trampa, Durazno, Talacasto, Las Crucecitas, Cerro Negro,

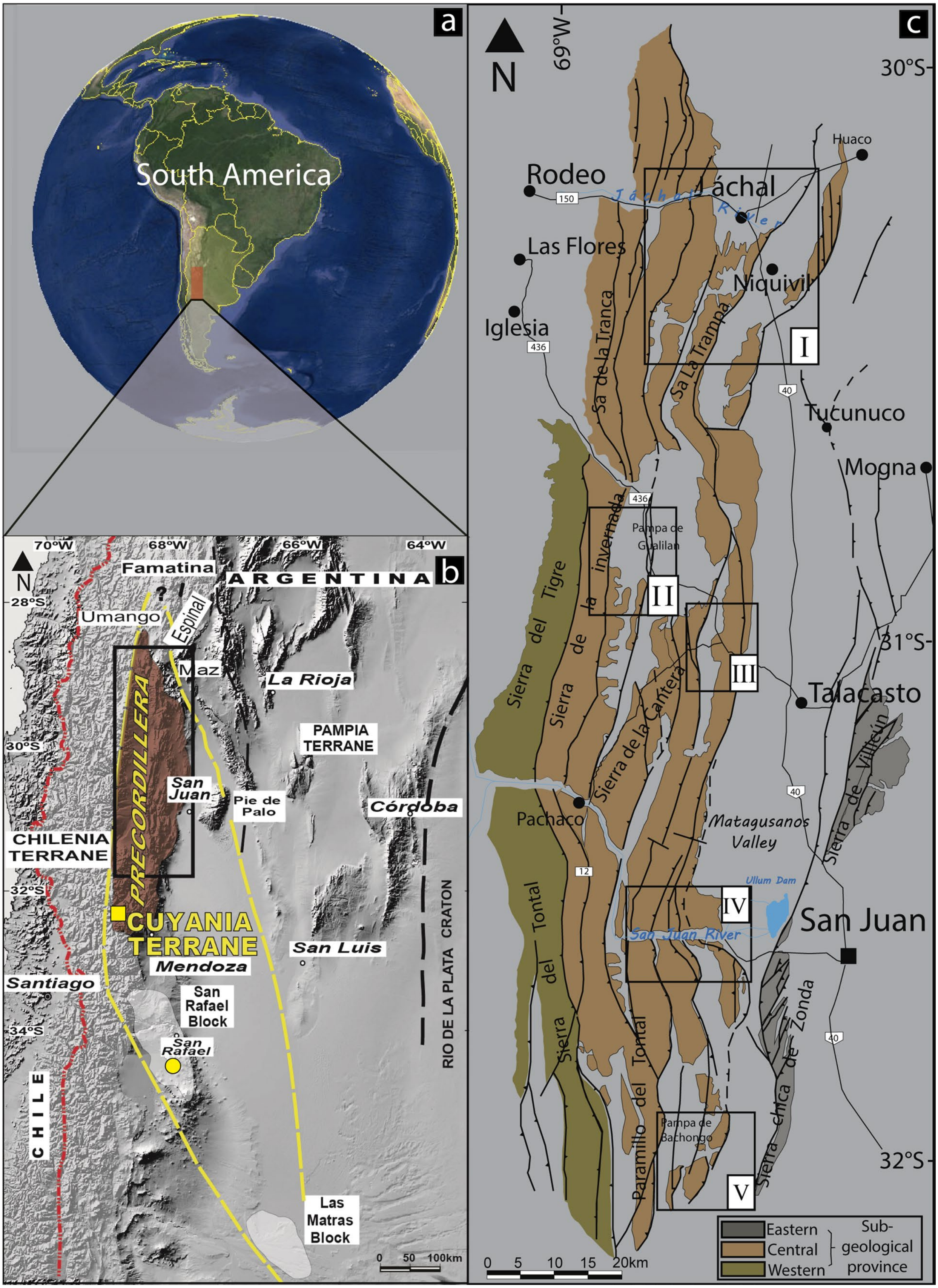
a
South America
b
70°W
68°W
66°W
64°W
N
Famatina
ARGENTINA
28°S
Umango
Espinal
Maz
La Rioja
PAMPIA TERRANE
30°S
PRECORDILLERA
San Juan
Pie de Palo
Córdoba
CHILENIA TERRANE
32°S
CUYANIA TERRANE
Mendoza
San Luis
Santiago
San Rafael Block
34°S
San Rafael
RIO DE LA PLATA CRATON
CHILE
Las Matras Block
0 50 100km
c
N
69°W
30°S
Huaco
Rodeo
150
Jáchal
Jáchal River
Las Flores
Niquivil
Iglesia
436
Sa de la Tranca
Sa La Trampa
I
40
Tucunuco
Mogna
436
Pampa de Gualilan
Sierra de la invernada
II
Sierra del Tigre
31°S
III
Talacasto
Sierra de la Cantera
Sierra de Villicún
40
Pachaco
Matagusanos Valley
12
Ullum Dam
Sierra del Tontal
IV
San Juan
San Juan River
Sierra chica de Zonda
40
Paramillo del Tontal
Pampa de Bachongo
32°S
V
Eastern
Central
Western
Sub-geological province
0 5 10 15 20km

La Chilca, Del Fuerte, among others. The Gualilán Group is in paraconcordance onto Silurian successions, either Tambolar Formation in the southern part of the basin or Los Espejos Formation in its central-northern area (Astini 1996; Astini and Maretto 1996). The Gualilán Group comprises the Talacasto (Padula et al. 1967) and the Punta Negra formations (Bracaccini 1949). Both units conform a Devonian sedimentary cycle (Baldis 1975) with main outcrops distributed in between the Jáchal River towards the north (30° S) and the San Juan River to the south (32º 31′ S) along the Central Precordillera (Fig. 2).

The *Talacasto Formation* was deposited on a marine shelf and is characterized by a transition from shale-dominated deposits at the base, towards bioturbated sandstones near the top of the unit (Baldis 1975; Astini 1991b; Keller 1999) with intercalated fine-grained sandstones and carbonate nodules (Astini 1990a). At Loma de los Piojos (Fig. 3f–h), the succession is 1145 m thick, whereas at the San Juan River area, it has a thickness of only *ca*. 100 m. The paleobiological content includes a rich association of

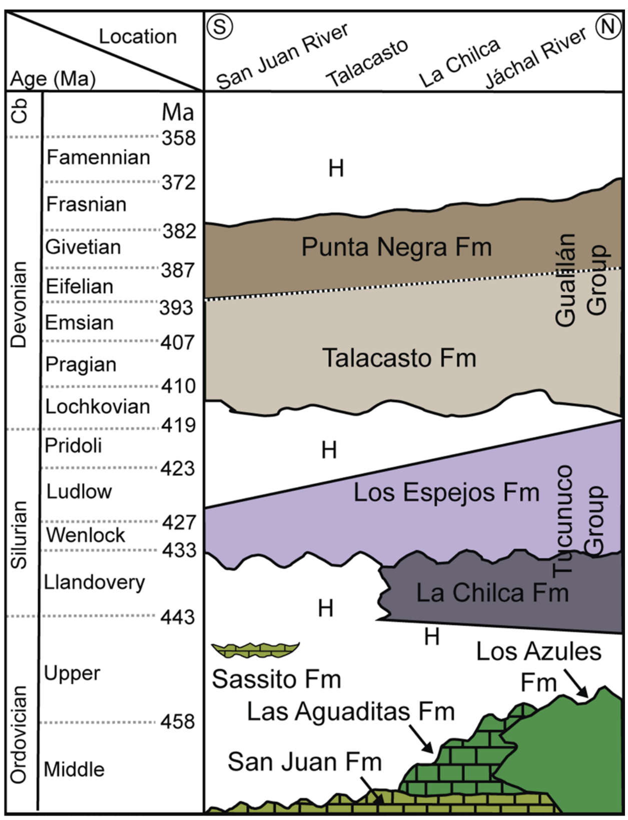

Fig. 2 Stratigraphic column with the different units showing the S to N diachronism of the Central Precordillera. *H* hiatus [modified from Astini (1996)]

marine invertebrates, largely brachiopods (Fig. 3i) linked to the Malvinokaffric fauna (Baldis and Rossi de García 1972; Amos and Boucot 1963; Herrera 1993, 1995a, b; Levy and Nullo 1970a, b; Racheboeuf and Herrera 1994; Racheboeuf et al. 1998; Sánchez et al. 1991; Rustán and Vaccari 2010; Carrera and Rustán 2015; Salas et al. 2013). Based on brachiopods Sánchez et al. (1991) and Herrera (1993) assigned an early Lochkovian age to the base of the unit (Fig. 2). A relevant ochre layer of approximately 10 m thick that can be traced more than 100 km in horizontal direction occurs in the central and northern sectors of the basin (Fig. 3g); the age of this bed is around the Pragian-Emsian boundary (Rustán 2011), as determined by its fossil record (essentially trilobites and brachiopods). This so-called "*Pleurotomaria* horizon" (Keidel 1921), is an excellent guide level within the Precordillera, demonstrating the diachronism of these units, which become younger towards the north (Herrera 1993; Rustán 2011).

The *Punta Negra Formation* paraconformably overlays the Talacasto Formation, and it is a thick succession of turbidite (flysch-like) deposits (Borrello 1969; González Bonorino 1975; Keller 1999) interpreted by Bustos and Astini (1997) as deposited in a fan-delta environment. It is composed of well-sorted sandstones, green greywackes, arkoses and shales and few conglomerates. Several sedimentary facies associations have been differentiated throughout the Punta Negra Formation (Edwards et al. 2009; Basilici et al. 2012) from which sandy beds with massive and amalgamated structures and heterolithic facies are dominant (Fig. 3a–c), some of them interpreted as a product of storm events on a shallow shelf (Bustos and Astini 1997; Poiré and Morel 1996). Trace fossils (Fig. 3d) of the *Nereites-Cruziana-Skolithos* ichnofacies are frequent (Peralta and Aceñolaza 1988; Peralta and Ruzicky 1990; Bustos 1996). Throughout the Devonian Punta Negra Formation, fragmentary plant debris are found (Fig. 3e). Species of plants described are *Sporogonites, Isidrophyton, Salopella, Haplostigma* (Edwards et al. 2009) and, more recently, *Haskinsia* (Arnol and Coturel 2017; Coturel and Arnol 2018). The paleoflora would have been transported from their presumed coastal and riverbank environment; the Lower-Middle Devonian assemblage gives further evidence of high-latitude vegetation (Edwards et al. 2001, 2009), and the age coincides with that previously defined by brachiopod fauna according to Herrera and Bustos (2001).

Paleocurrent studies in this unit show a predominance of east–west flow direction (González Bonorino 1975; González Bonorino and Middleton 1976; Bustos 1995; Vieira de Luca and Basilici 2008, 2013; Basilici et al. 2012), with an average movement vector of the flow between 260° and 275° and standard deviations below 38° in all cases (Bustos 1995).

Sampling and methodology

The Gualilán Group was studied in five different sections covering all the areal development of the basin, both in a north–south and east–west directions (Figs. 4, 5). Descriptions of the selected sedimentological sections were made during fieldworks. All lithological types of the Gualilán Group were sampled. To obtain relevant information regarding each succession, we carried out studies of petrography, heavy minerals, whole-rock geochemistry, Sm–Nd isotopic ratios and U–Pb detrital zircon dating (Table 1).

Sandstone petrography

A total of 11 thin sections of sandstones were studied under the microscope and quantitatively analysed with a Swift-type point counter. 400 points were counted using the traditional method of Gazzi-Dickinson (Ingersoll et al. 1984) and accordingly, plutonic rock fragments were counted as such, rather than as mineral components. The results were plotted in Q-F-L ternary diagrams (Dickinson et al. 1983). The populations represented in each triangle include detrital grains, except for micas, opaque minerals, chlorite, heavy minerals and carbonate grains. Chert was counted as a sedimentary rock fragment.

Heavy mineral analysis

Heavy mineral concentrates were obtained from psammitic samples weighing approximately 5 kg, following conventional crushing, milling and sieving; identification and final separation by hand-picking was achieved using a binocular microscope. An electron microscope with EDAX (Philips SEM 505) at Centro de Investigación y Desarrollo de Ciencias Aplicadas (CINDECA, La Plata) helped with the identification of heavy mineral species. One sample from each unit taken at the Talacasto Creek section (16T45 and 16PN43) provided the detrital zircon grains for morphological studies following Pupin (1980): $n = 37$ for the Talacasto Formation and $n = 40$ for the Punta Negra Formation. Multiple parameters such as crystal habit (shape), size, elongation, roundness and surface features were examined under the scanning electron microscope (JEOL JSM 6360 LV) at the Museo de La Plata, to determine their morphological and typological parameters to infer source rock types (Gärtner et al. 2013).

Lithogeochemistry

Whole-rock geochemistry of sedimentary rocks reflects the average composition of the crust that shed detritus to a certain basin (Taylor and McLennan 1985). However, weathering, hydraulic sorting and diagenesis acting from initial erosion of a source rock(s) to the final burial of detritus may modify the signatures of the source rock(s), and therefore, these factors require evaluation to constrain the provenance of a sedimentary succession (Nesbitt and Young 1982; Nesbitt et al. 1996). Fine-grained rocks are the most appropriate for provenance studies because of the sensibility on the mobility of some elements to particle sizes during deposition and diagenesis (Cullers 1995). Ten pulp samples of shales and mudstones were prepared and analysed at ACME Labs, Canada (Table 1). Major elements were obtained by inductively coupled plasma emission spectroscopy (ICP-ES) on fusion beads (Table 2). Loss on ignition (LOI) was determined by igniting a sample split and measuring the weight loss. Rare earth elements (REE) and certain trace elements were analysed by inductively coupled plasma mass spectrometry (ICP-MS; Tables 3 and 5).

Whole-rock Sm–Nd isotopes

Sm–Nd isotopes are widely used as provenance indicators (e.g., McLennan et al. 1990, 1993). Nd isotopic signatures of terrigenous sedimentary rocks are the average of the signatures of the various sources from which the sediments were derived (McLennan 1989). Since the Sm/Nd ratio is modified during processes of mantle–crust differentiation it is possible to estimate the time at which the initial magma was separated from the upper mantle, also called the depleted mantle model age or T_{DM} (DePaolo 1981). The model age of sedimentary rocks should be interpreted as the model ages of those rocks which have contributed to a higher degree to the Sm–Nd ratio of that sediment.

Whole-rock powders were spiked with a tracer and completely dissolved using acids, followed by column procedures using cationic and anionic resins to obtain the Sm and Nd. The isotopic determinations were performed using static mode on a VG sector 54 multi-collector TIMS at the Laboratory of Isotope Geology CPGeo-USP, Brazil (Table 1). The $\varepsilon_{Nd(t)}$ indicates the deviation of the $^{143}Nd/^{144}Nd$ value of the sample from that of CHUR or Chondritic Uniform Reservoir (DePaolo 1981). All Sm/Nd data are shown in the supplementary material.

U–Pb detrital zircon analyses

Three samples from each formation of the Gualilán Group as depicted in Table 1 were analysed by U–Pb geochronology

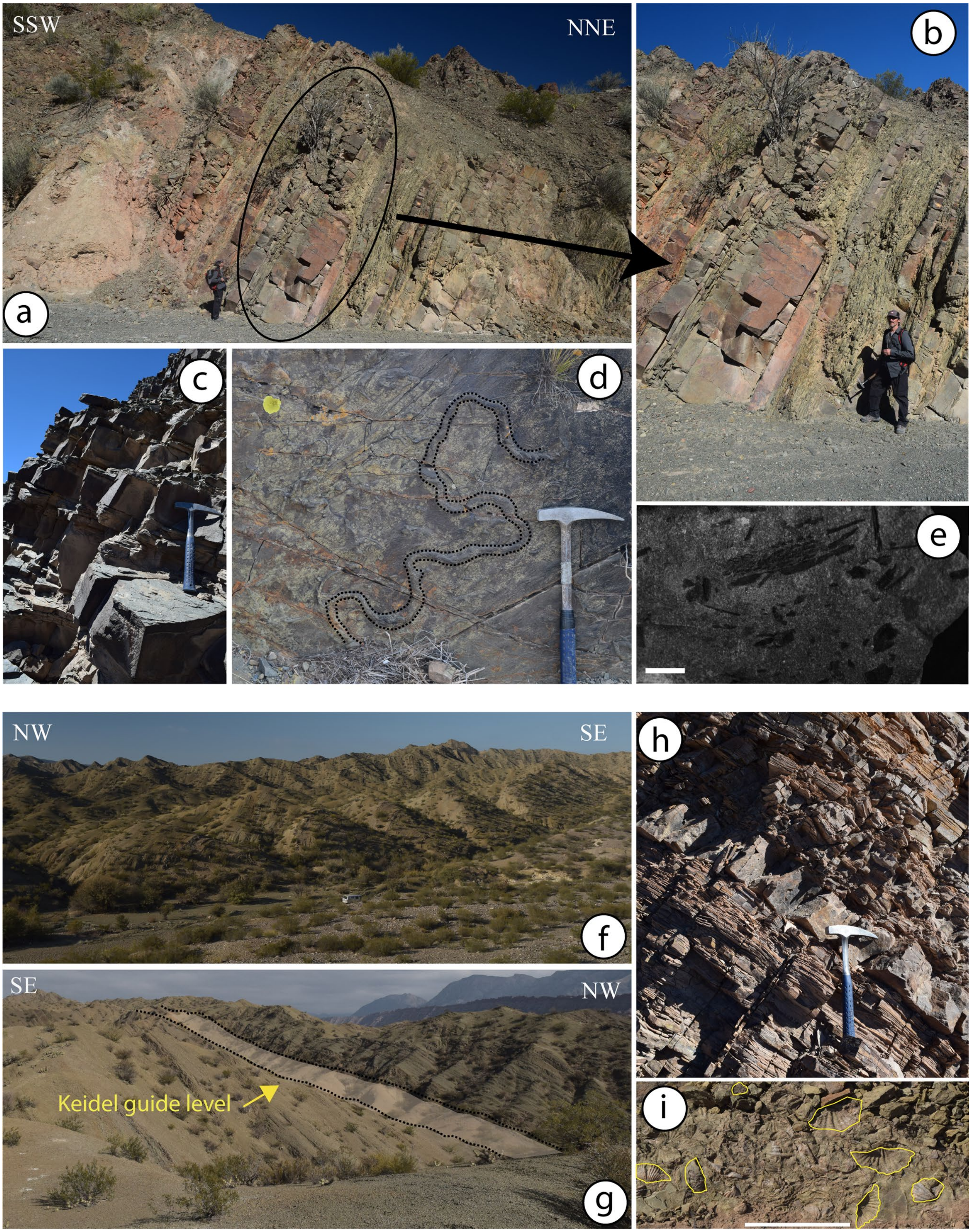
SSW
NNE
a
b
c
d
e
NW
SE
f
SE
NW
Keidel guide level
g
h
i

◂**Fig. 3** Field photographs of the studied units. Punta Negra Formation: **a**, **b**, **c** Outcrops with the psammitic facies above the pelitic facies in San Juan River. **d** Trace fossil. **e** Plant debris, scale bar = 1 cm. Talacasto Formation: **f**, **g** Regional photographs of the outcrops near Jáchal. **h** Sedimentary succession with the predominance of the pelitic over the psammitic facies. **i** Brachiopods of the *Malvinokaffric* fauna, scale bar = 10 cm

using a laser ablation (LA) system coupled to an ICP-MS (Neptune), following the methodology after Sato et al. (2010). Zircon grains were mounted in 2.5 cm-diameter circular epoxy mounts and polished down until they were revealed. The internal texture of each grain was observed using cathodoluminescence (CL) images. The percentage of common Pb was dismissed during data processing; $^{206}Pb/^{268}U$ and $^{207}Pb/^{235}U$ ratios were established, and zircons with 100 ± 10% degree of concordance were used. The data are portrayed in Concordia or Tera-Wasserburg diagrams generated with the programme Isoplot/Ex (Ludwing 2001). All these procedures were performed at the Centro de Pesquisas Geocronológicas, Universidade de Sao Paulo, Brazil. All LA-ICP-MS zircon data are shown in the supplementary material.

Results

Sandstone petrography

Petrographical analysis of sedimentary rocks is useful as a first approach to provenance studies (Dickinson et al. 1983). Results can be enhanced by geochemical and isotope analyses, considering that only the more stable minerals survive weathering and diagenesis.

Talacasto Formation the five samples analysed are well-sorted, fine-grained sandstones with angular to subangular clasts. Sandstones from the southern sector of the basin show a pervasively altered pseudomatrix and hence a submature texture. Sandstones from the northern sector instead are texturally mature because of the absence (or very scarce) matrix content. Monocrystalline quartz is dominant with normal or undulose extinction and corroded edges. Inclusions of different minerals are occasionally found in quartz, being acicular rutile the commonest. Grain size decreases from south to north, and so the abundance of polycrystalline quartz.

Feldspar is a minor clastic constituent in samples from the central and northern parts of the basin. Plagioclase (around 3%) is present in all samples, showing polysynthetic twinning and slightly altered edges; numerous crystals have a deformed twinning pattern (Fig. 6). Alteration of Potassium feldspar is strong, and carbonate completely replaced some grains. Lithoclasts become more abundant towards the south of the basin; they are mostly of metamorphic origin and contain sparse feldspar. Among the accessory minerals, phyllosilicates are abundant: detrital biotite is squeezed in between resistant minerals and muscovite is finer and less deformed. Very fine-grained white mica and chlorite are present as cement or disseminated crystals. Translucent heavy minerals include zircon, apatite, tourmaline, rutile, epidote among others. An exception is sample 16T56, because it is a medium-grained sandstone predominantly composed of mono- and polycrystalline quartz, and metamorphic lithoclasts. Euhedral reddish crystals, often in aggregates, were preliminarily identified as spinel. Brachiopod shells of *Australospirifer*? and *Australocoelia palmate* of calcitic composition were determined. Palynomorphs are also recognized, but to further determine them is beyond the scope of this work (Fig. 6).

Punta Negra Formation six samples of medium to fine-grained, moderately well-sorted sandstones were analysed (Fig. 6). Detrital grains are subangular to subrounded, and the matrix is less than 15% in all samples. Monocrystalline quartz prevails, showing undulose extinction, slightly dissolved edges, and sometimes displaying mineral inclusions. Polycrystalline quartz is considerably abundant, reaching 25% in some samples. Metamorphic lithoclasts derived from schists are the second component in order of abundance, and less common are felsic lithoclasts sourced from volcanic and plutonic rocks. The third component in order of abundance is potassium feldspar showing edges altered to sericite; microcline and exsolved perthitic feldspar are present. As set out for the Talacasto Formation, plagioclase show distorted twin lamellae and, in some cases, they are altered at edges or inside the crystal (Fig. 6). Detrital biotite and muscovite are common. Biotite is very deformed, whereas muscovite tends to be shorter, tabular and preserves its original shape. Detrital and authigenic chlorite is markedly present. Muscovite, chlorite and feldspars define banded microstructures. Translucent heavy minerals include zircon, tourmaline, rutile, garnet, epidote, monazite and spinel. Hematite and magnetite are also present. The matrix is predominantly composed of quartz, K-feldspar and plagioclase. The cement is rich in clay minerals with occasional carbonate.

In the Q-F-L ternary diagram the samples from both units plot in the recycled orogen field. In the Qm-F-Lt diagram samples from the Talacasto Formation indicate a mixed provenance, whereas those from the Punta Negra Formation plot in the transitional recycled field (Fig. 7).

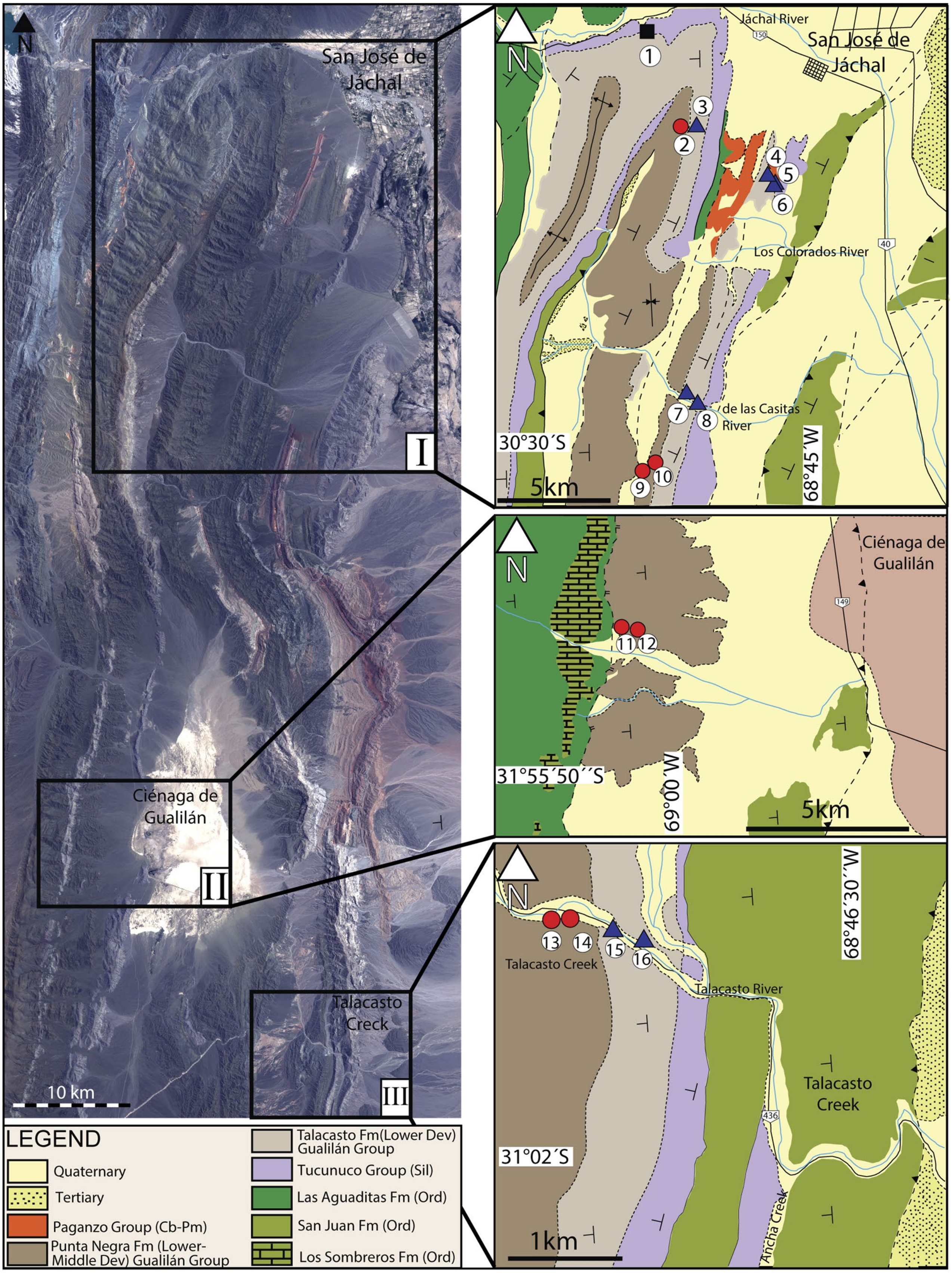

N
San José de Jáchal
I
Ciénaga de Gualilán
II
Talacasto Creek
III
10 km
Jáchal River
150
San José de Jáchal
Los Colorados River
40
de las Casitas River
30°30´S
68°45´W
5km
Ciénaga de Gualilán
149
31°55´50´´S
69°00´W
5km
Talacasto Creek
Talacasto River
68°46´30´´W
Talacasto Creek
436
Ancha Creek
31°02´S
1km
LEGEND
Quaternary
Tertiary
Paganzo Group (Cb-Pm)
Punta Negra Fm (Lower-Middle Dev) Gualilán Group
Talacasto Fm(Lower Dev) Gualilán Group
Tucunuco Group (Sil)
Las Aguaditas Fm (Ord)
San Juan Fm (Ord)
Los Sombreros Fm (Ord)

◂**Fig. 4** Northern Precordillera studied areas, San Juan province. Samples: "blue coloured triangle" Talacasto Formation; "red coloured circle" Punta Negra Formation; "black coloured square" Los Espejos Formation

Heavy mineral analysis

The morphology of zircon can be greatly affected as a result of long transport and reworking during a sedimentary cycle (Dickinson and Gehrels 2003), morphological studies are useful as broad indicators of source rock types (Pupin 1980). The occurrence of zircon with different morphologies in sandstones is usually indicative of source mixing.

The detrital heavy mineral assemblage of the Talacasto Formation comprises zircon, tourmaline, rutile, epidote, apatite, garnet, staurolite, chromian spinel and magnetite (Fig. 8). Samples of the Punta Negra Formation comprise the aforementioned minerals accompanied by monazite and titanite; unlike the Talacasto Formation, spinel are rather absent.

Zircon morphology

Zircon is widely used in provenance studies, and it is the most abundant accessory mineral of the Gualilán Group. From the same samples used for U–Pb zircon dating of both formations, we randomly selected crystals to analysed their morphology.

Zircon crystals classify in three main morphological groups and several families. Group 1 comprises 30 and 35% of the crystals (from the Punta Negra and Talacasto formations, respectively), showing short prismatic shapes with bipyramidal faces and simple facets indicating derivation from plutonic sources. Group 2 includes 60 to 62% of the crystals (from the Talacasto and Punta Negra formations, respectively), showing short prismatic, multifaceted shapes and correspond to grains associated with a probable metamorphic event. Rounded crystals not ascribed to a particular morphology evidencing long history of transport and recycling from a craton interior sum up 2.7% for the Talacasto, and 10% for the Punta Negra formations (Fig. 9).

Lithogeochemistry

The geochemical composition of sedimentary rocks depends fundamentally on the nature of the sources from which they derive, and on the processes they experienced, such as weathering, transport, and subsequent deposition and diagenesis.

The low mobility of some trace elements and REE during deposition and diagenesis make the fine-grained sandstone and claystone the most appropriate rocks for provenance analysis based on geochemistry (Cullers 1995); it is a valuable tool to decipher the provenance of matrix-rich sandstones and wackes. Because ratios of certain trace elements and REE remain largely unchanged from source to sink they are used in numerous diagrams to determine, for instance, the average chemical composition of the set of source rocks that provided debris to the sedimentary rocks under study. Particularly useful are the ratios between compatible and incompatible elements (i.e., Zr/Sc, Th/Sc), although ratios between elements of the same compatibility (i.e., Cr/V, La/Th) are also helpful (McLennan et al. 1993). Specific ratios such as Th/Sc and the type of the Eu-anomaly (positive, negative or absent), are also important indicators of the composition of the source rocks, particularly when compared to the Upper Continental Crust (UCC) average values (McLennan et al. 1993).

Sorting and weathering

Both units of the Gualilán Group display a similar distribution of major elements (Table 2). A sample from the Silurian Los Espejos Formation is used for comparison, and it is noteworthy that it shows similar values, except for a lower concentration of SiO_2, a higher concentration of Al_2O_3 and a notable amount of P_2O_5 (2 wt%).

The chemical index of alteration (CIA) helps to evaluate the degree of weathering of the analysed rocks. Samples from the Gualilán Group (Talacasto and Punta Negra formations) show CIA values between 71.1 and 75.9 (Table 2), implying a moderate weathering. The sample 16LE29 (Los Espejos Formation) has a CIA value of 67.9 (Table 2), therefore, in the same range of weathering.

In the A-CN-K diagram (Fig. 10a; Fedo et al. 1995), both units studied show a normal weathering trend from average granite composition (more felsic than average UCC).

During weathering and recycling, there is a tendency for an elevation of the Th/U ratio above upper crustal igneous values of 3.8–4.0. This is because under oxidizing conditions U^{+4} oxides to the more soluble U^{+6} becoming more easily removed from sediments than Th (McLennan et al. 1993). Samples from the Talacasto Formation show Th and U averages of 14.04 ppm and 3.06 ppm, whereas the Punta Negra Formation display average values of 14.1 ppm and 3.4 ppm, respectively (Table 3), being, therefore, essentially similar to Post-Archaean Australian Shales (PAAS) averages (Th = 14.6 ppm and U = 3.1 ppm). In the Th/U vs.

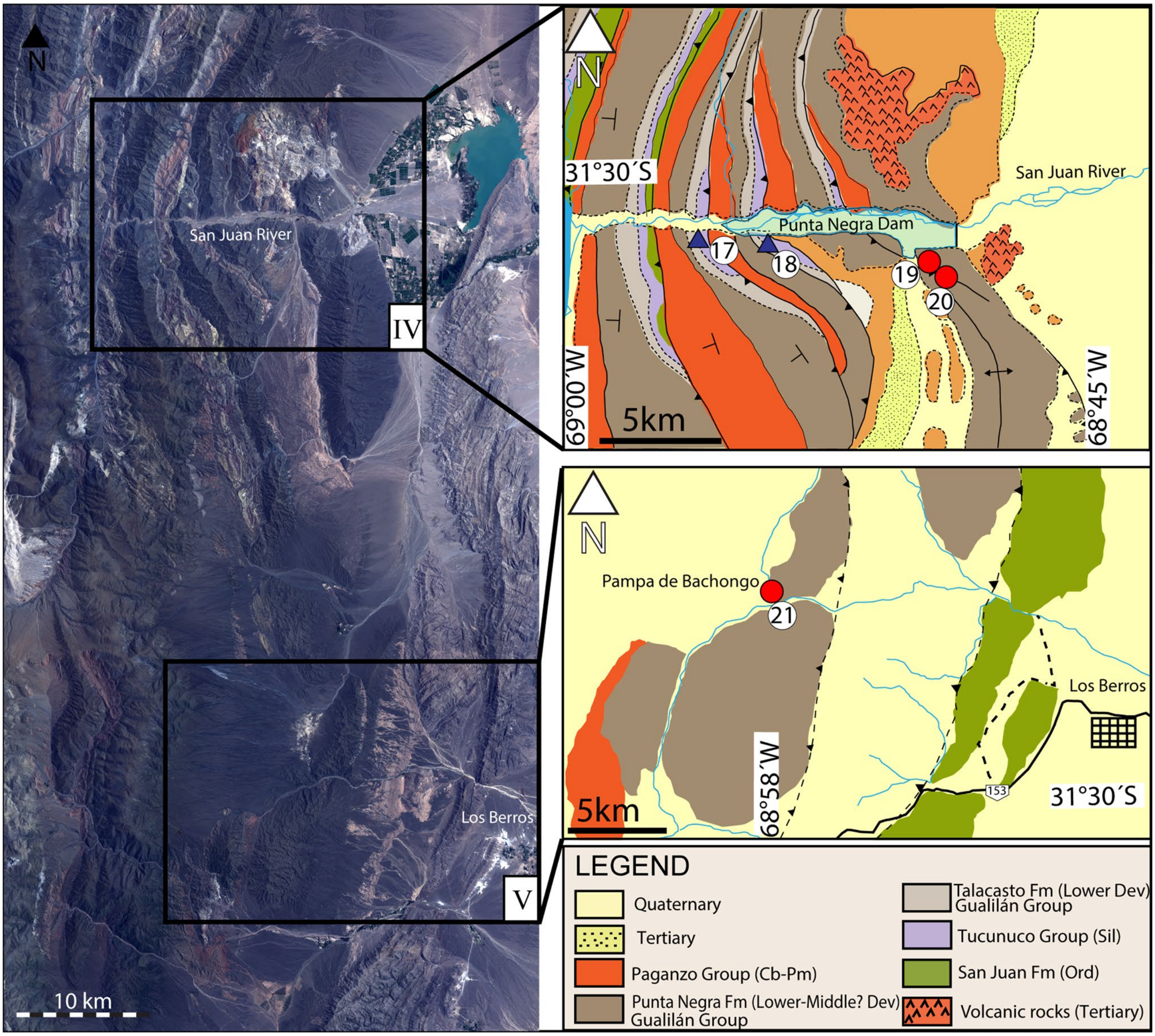

Fig. 5 Southern Precordillera studied areas, San Juan province. Samples: "blue coloured triangle" Talacasto Formation; "red coloured circle" Punta Negra Formation

Th diagram, the samples analysed from the Gualilán Group show a derivation from average UCC (Fig. 10b1) and, therefore, in coincidence with CIA values indicate moderate weathering (Table 1).

Source composition

Due to the immobile behaviour of the trace elements (particularly high field strength elements), they are useful for provenance analysis, since they preserve characteristics of the source rocks and, therefore, reflect provenance compositions. Ratios such as Th/Sc, Zr/Sc and Cr/V, along with the REE distribution pattern, provide some of the most useful data for provenance determination (Taylor and McLennan 1985).

Zr/Sc vs Th/Sc are useful for provenance analyses. Samples from the Gualilán Group show Th/Sc ratios ranging from 0.68 to 0.83, whereas the Zr/Sc ratios vary between 8.58 and 18.23 (Table 4). In the Zr/Sc vs Th/Sc diagram (Fig. 10b2) it is evident that reworking was insignificant and

Table 1 Number, rock type, analyses and geographical coordinates of samples

Units	Number	Rock type	Sample	Geographic coordinates	Methodologies
Punta Negra Fm (Lower-Middle Devonian)	9	Sandstone	16PN33	30°31′07.00″S 68°52′39.00″W	Petrography, U/Pb
	10	Shale/Mudstone	16PN34	30°31′07.00″S 68°52′39.10″W	Geochemistry, Sm/Nd
	13	Sandstone	16PN43	30°0.1′00″S 68°47′38.00″W	Petrography, U/Pb, Zr Morphology
	14	Shale/Mudstone	16PN44	30°0.05′00″S 68°43′34.00″W	Geochemistry, Sm/Nd
	11	Shale/Mudstone	16PN52	30°50′48.68″S 69°0′46.54″W	Geochemistry
	12	Sandstone	16PN54	30°50′50.79″S 69°0′55.23″W	Petrography
	19	Shale/Mudstone	16PN58	31°32′54.53″S 68°49′58.29″W	Geochemistry
	20	Sandstone	16PN59	31°32′0.49″S 68°49′42.74″W	Petrography
	2	Sandstone	17PN07	30°17′50.28″S 68°50′53.64″W	Petrography, U/Pb
	21	Sandstone	17PN18	31°53′45.18″S 68°49′35.46″W	Petrography
Talacasto Fm (Lower Devonian)	3	Sandstone	17T04	30°18′11.88″S 68°50.4′80″W	Petrography, U/Pb
	4	Shale/Mudstone	16T08	30°17′04″S 68°46′51.00″W	Geochemistry, Sm/Nd
	6	Shale/Mudstone	16T11	30°31′32″S 68°54′11.00″W	Geochemistry, Sm/Nd
	7	Shale/Mudstone	16T38	30°17′47.00″S 68°46′33.00″W	Geochemistry, Sm/Nd
	8	Sandstone	16T40	30°28′4.35″S 68°50′10.00″W	Petrography, U/Pb
	15	Sandstone	16T45	31°0′9.99″S 68°46′50.00″W	Petrography, U/Pb, Zr Morphology
	16	Shale/Mudstone	16T46	31°0′10.00″S 68°46′50.00″W	Geochemistry, Sm/Nd
	5	Sandstone	16T56	31°17′39.10″S 68°46′42.56″W	Petrography
	17	Sandstone	16T64	31°31′54.63″S 68°54′53.29″W	Petrography
	18	Shale/Mudstone	16T65	31°31′54.63″S 68°54′53.15″W	Geochemistry
Los Espejos Fm (Silurian)	1	Shale/Mudstone	16LE29	30°12′35.25″S 68°53′7.90″W	Geochemistry, Sm/Nd

The number is related to Figs. 4, 5

Table 2 Major elements (expressed in wt%) of shales and mudstone samples from the Gualilán Group, including CIA values

Formation	Sample	SiO_2	Al_2O_3	Fe_2O_3	MgO	CaO	Na_2O	K_2O	TiO_2	P_2O_5	MnO	LOI	Sum	CIA
Punta Negra	16PN34	57.92	19.08	7.57	2.59	0.53	1.15	4.39	0.99	0.15	0.06	5.3	99.81	75.9
	16PN44	54.12	18.92	9.26	3.78	1.56	1.99	4.15	1.07	0.18	0.09	4.5	99.77	71.1
	16PN52	54.28	19.58	8.32	2.61	1.27	1.25	4.56	1.08	0.21	0.07	6.5	99.80	73.4
	16PN58	55.82	19.05	8.67	3.23	0.70	1.79	4.59	1.01	0.26	0.09	4.5	99.79	72.9
Talacasto	16T08	59.14	18.64	7.29	2.12	0.84	1.31	4.04	0.85	0.13	0.07	5.3	99.83	75.1
	16T11	61.86	16.60	7.08	2.24	1.03	1.67	3.32	0.92	0.18	0.06	4.8	99.84	73.4
	16T38	58.24	18.41	8.34	2.52	0.81	1.46	3.81	0.94	0.17	0.07	5.0	99.82	75.2
	16T46	65.74	14.86	6.56	1.98	0.88	1.80	3.05	0.90	0.16	0.05	3.8	99.81	72.2
	16T65	59.28	18.55	7.93	2.59	0.39	1.43	4.19	0.96	0.10	0.12	4.2	99.80	75.5
Los Espejos	16LE29	51.01	20.45	7.85	2.74	3.35	1.60	4.71	0.88	2.1	0.09	4.9	99.75	67.9
	UCC	65.89	15.17	4.49	2.2	4.19	3.89	3.39	0.5	0.2	0.07		99.98	56.9

that the lack of Th and Zr enrichments suggest derivation from unrecycled average UCC; in Fig. 10b2 the fine-grained samples (shales and mudstones) plot towards the UCC line. The Los Espejos Formation shows a pattern similar to the Gualilán Group, with Th/U of 3.95, Zr/Sc of 7.9 and Th/Sc of 0.69.

Cr/V vs Y/Ni (Fig. 10c1) and La/Th vs Hf (Fig. 10c2) diagrams help to strengthen a derivation from felsic unrecycled sources for the sediments that filled the Devonian basin in the Precordillera region. La/Th ratios varying between 1.91 and 3.25 (Table 5) are similar to UCC (red square). The Silurian Los Espejos Formation was probably also fed by a felsic source; the high Y/Ni ratio of 2.55 is presumably linked to the presence of apatite.

The shape of the REE patterns can provide information about both, bulk compositions and nature of the source

Table 3 Trace elements (expressed in ppm) of shales and mudstone samples from the Gualilán Group and the Silurian Los Espejos Formation for comparison

Formation	Sample	Ba	Ni	Sc	Be	Co	Cs	Ga	Hf	Nb	Rb	Sn	Sr	Ta
Punta Negra	16PN34	578	50	20	4	15.2	9.1	23.2	5.1	16.2	190.9	4	63.6	1.3
	16PN44	763	56	19	4	23.9	3.8	25.6	6.4	17.2	156.7	3	154.8	1.3
	16PN52	648	61	22	4	18.7	9.3	24.7	5.5	17.3	196.1	4	87.3	1.3
	16PN58	705	44	19	4	19.3	5.0	25.4	6.2	17.0	176.1	4	91.1	1.2
Talacasto	16T08	693	34	19	3	17.0	8.8	23.7	4.6	16.6	179.6	4	71.1	1.3
	16T11	455	53	18	4	17.5	6.7	20.3	6.2	16.3	141.5	4	73.9	1.5
	16T38	501	42	20	3	15.6	7.5	22.9	4.8	16.3	168.5	4	66.7	1.5
	16T46	411	41	15	3	16.5	5.9	16.0	7.1	14.9	131.2	3	84.5	1.4
	16T65	436	48	20	3	20.1	9.1	22.2	5.6	16.8	186.1	4	59.0	1.2
Los Espejos	16T29	625	45	23	5	17.3	11.1	26.8	5.0	15.8	209.6	4	101.8	1.2
Formation	Sample	Th	U	V	W	Zr	Y	Mo	Cu	Pb	Zn	As	Bi	Cr
Punta Negra	16PN34	14.3	3.3	168	14.6	177.4	29.3	0.6	48.2	17.7	134	1.8	0.4	115.9
	16PN44	13.0	3.3	152	27.8	230.7	38.7	0.4	51.7	15.1	152	5.0	0.3	109.4
	16PN52	14.9	3.6	185	1.8	192.9	38.7	0.9	51.4	18.5	146	6.7	0.5	123.9
	16PN58	14.2	3.5	145	1.8	215.9	46.8	0.5	58.4	17.0	166	2.3	0.3	88.4
Talacasto	16T08	15.8	3.4	164	29.9	163.1	32.1	1.2	37.0	23.2	119	14.2	0.7	82.0
	16T11	13.3	2.9	139	73.4	223.1	32.5	0.8	31.3	15.7	112	6.1	0.4	82.0
	16T38	13.6	2.8	159	29.4	179.3	34.4	0.6	35.2	17.6	135	3.3	0.5	95.4
	16T46	12.4	3.1	131	81.6	273.5	32.6	1.1	22.8	12.7	100	10.0	0.2	82.5
	16T65	15.1	3.1	201	2.5	197.1	32.6	bdl	30.5	16.9	147	1.4	0.5	96.4
Los Espejos	16T29	15.8	4.0	204	25.6	181.7	114.6	1.3	34.0	19.8	119	5.7	0.6	95.8

bdl below detection limit

(McLennan and Taylor 1991). The chondrite-normalized REE diagram for the Gualilán Group shows a moderately enriched light rare earth elements (LREE) pattern, a negative Eu-anomaly, and a rather flat heavy rare earth elements (HREE) distribution (Fig. 10d), being, therefore, essentially similar to the PAAS (Nance and Taylor 1977) and to the UCC (Rudnick and Gao 2003). As depicted in Fig. 10d, the sample 16LE29 from the Silurian Los Espejos Formation shows enrichment in REE compared to the Gualilán Group.

Isotope geochemistry

The Sm–Nd isotope system is a good provenance indicator, since it aids in the determination of the grade of fractionation and the average crustal residence time of the detrital mix (McLennan et al. 1990). This is because the system is usually not reset by processes operating during erosion, sedimentation and metamorphism (DePaolo 1981; McDaniel et al. 1997; Goldstein et al. 1997).

Samples of the Talacasto Formation (t = *ca.* 410 Ma, biostratigraphic age) show T_{DM} ages between 1.40 and 1.46 Ga (Early Mesoproterozoic) and $\varepsilon_{Nd(t)}$ values ranging from − 9.83 to − 10.36 (Fig. 11). The Punta Negra Formation ($t = ca.$ 390 Ma, biostratigraphic age) displays T_{DM} ages between 1.45 and 1.5 Ga (Early Mesoproterozoic), whereas $\varepsilon_{Nd(t)}$ values range from − 9.21 to − 11.13 (Fig. 11). A single data from Los Espejos Formation (t = *ca.* 423 Ma), has a model age of 2.2 Ga (Paleoproterozoic) and $\varepsilon_{Nd(t)}$ of − 7.65, but isotopic fractionation cannot be completely ruled out based on a single data (Fig. 11).

U/Pb detrital zircon ages

Detrital zircon dating gives insights regarding felsic source rocks ages, and guide the understanding of continental crust growth and recycling (Fedo et al. 2003). We sampled both formations of the Gualilán Group at each locality of the study area (Fig. 12).

At the section of Las Aguaditas Creek (Fig. 13), the sample from the Talacasto Formation (17T04; $N = 94$) is characterized by a dominance (37.2%) of detrital zircon grains with ages ranging from 975 to 520 Ma (Neoproterozoic–Early Cambrian), derived from rocks of the Pampean–Brazilian orogenic cycle. The Famatinian (Middle/Late Cambrian-Devonian) and Grenvillian-Sunsas (Mesoproterozoic) orogenic cycles are represented by 27.7% of the detrital zircon each, with an age range between 519–427 and

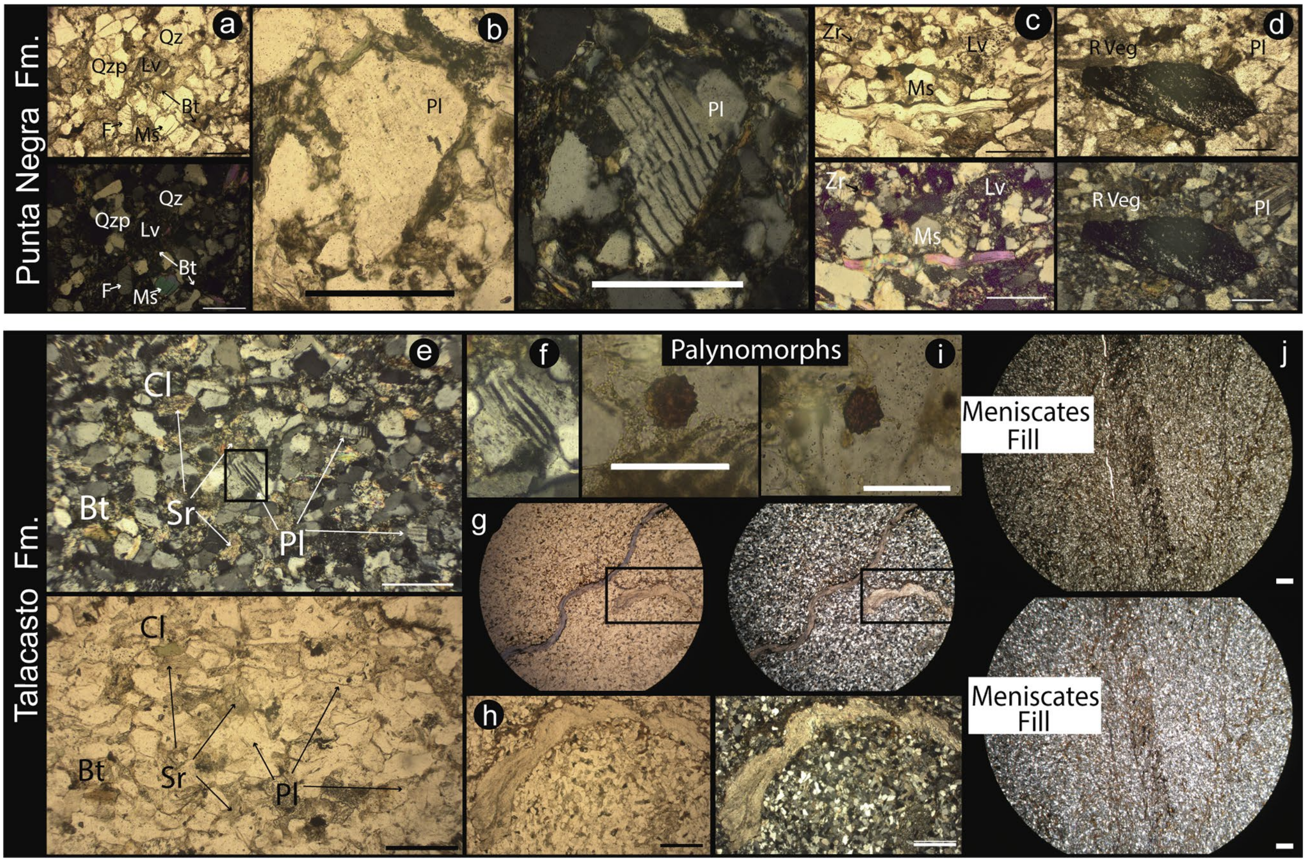

Fig. 6 Microphotographs of rock samples from the Punta Negra (**a**, **b**, **c**, **d**) and Talacasto (**e**, **f**, **g**, **h**, **i**, **j**) formations. *Qz* quartz, *Qzp* polycrystalline quartz, *Pl* plagioclase, *F* K-feldspar; *L* lithoclasts, *Lv* volcanic lithoclasts, *Ms* muscovite, *Bt* biotite, *Zr* zircon, *Cl* chlorite, *Sr* sericite, *R veg* plant debris. Scale bar = 100 µm

1494–1055 Ma, respectively. The oldest zircons are from the Transamazonian (Paleoproterozoic) orogenic cycle, with 7.4% of the ages between 1896 and 1608 Ma.

The main peak of detrital zircon ages of the Punta Negra Formation (17PN07; $N = 69$) is Mesoproterozoic (53.5%), with ages ranging from 1472 to 1014 Ma, 56.7% are Stenian (1193–1014 Ma). The second peak in order of abundance (28.2%) comprises ages of Pampean–Brazilian orogenic cycle, including Early Cambrian (521–536 Ma) and Neoproterozoic ages (577–996 Ma). A third cluster (12.7%), with an age range from 517 to 400 Ma records the Famatinian (Middle/Late Cambrian–Devonian) orogenic cycle. The oldest detrital zircon ages are Paleoproterozoic (5.6%; 1953–1617 Ma).

At the Río de las Casitas section (Fig. 14), the Talacasto Formation (16T40; $N = 20$), shows 38.1% of detrital zircon with Mesoproterozoic ages ranging from 1383 to 1018 Ma. The Pampean–Brazilian orogenic cycle (Neoproterozoic–Early Cambrian) records 33.3% of ages between 953 and 544 Ma, whereas Famatinian ages (28.6%) cluster between 515 and 397 Ma.

The Punta Negra Formation, represented by sample 16PN33 ($N = 105$), is characterized by 60% of Mesoproterozoic zircon grains. This population comprises 66.6% of Stenian ages (1194–1010 Ma), 25.4% of Ectasian ages (1348–1202 Ma), and 8% of Calymmian ages (1505–1405 Ma). Famatinian ages (30.5%) are dominated by Ordovician detrital zircon grains (484–453 Ma, 82%), and minor Middle and Late Cambrian (485–518 Ma), Silurian (429 Ma) and Devonian (417 Ma) zircon dates. The Pampean–Brazilian orogenic cycle (Neoproterozoic–Early Cambrian) is represented by 6.2% of the analysed zircon,

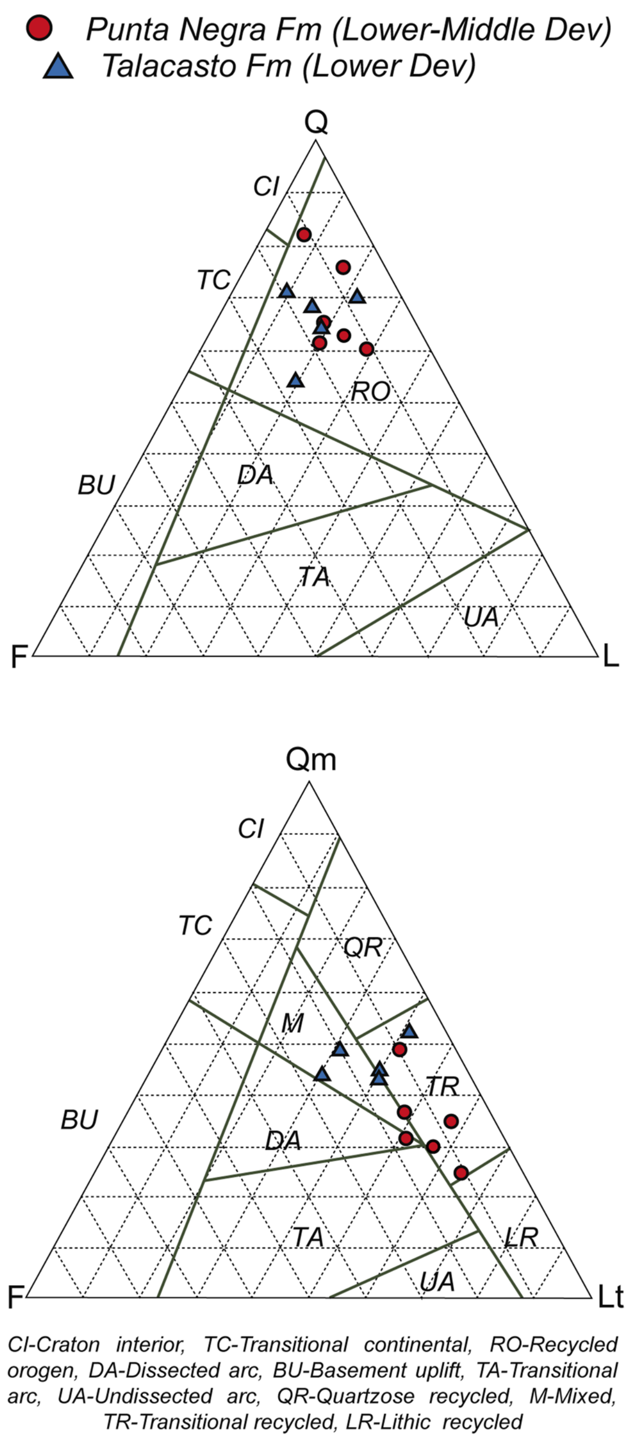

Fig. 7 Provenance ternary diagrams after Dickinson et al. (1983) showing distribution of the sandstone samples from the Gualilán Group. *F* feldspar, *Qt* total quartz, *Lt* total lithoclasts (including polycrystalline quartz), *Qm* monocrystalline quartz, *L* lithoclasts

with ages between 946 and 525 Ma. The age of 1810 Ma is assigned to the Transamazonian orogenic cycle, whereas detrital zircon grains in the age range of 2588–2564 Ma are derived from Archean sources.

At the Talacasto Creek (Fig. 15), the Talacasto Formation (sample 16T45; $N=80$) displays two main populations represented by 37.5% of detrital zircon grains. One population is Mesoproterozoic with ages between 1579–1061 Ma (Grenvillian-Sunsas orogenic cycles), whereas the other one records the Pampean–Brazilian orogenic cycle (Neoproterozoic–Early Cambrian), with ages between 848–521 Ma. The Famatinian orogenic cycle (Middle/Late Cambrian–Devonian) with 16.3% of the total grains, comprises Late Cambrian (519–491 Ma) and Ordovician (480–467 Ma) ages. The Paleoproterozoic ages (8.8%) range between 2133 and 1624 Ma.

The Punta Negra Formation is represented by sample 16PN43 ($N=87$) and shows conspicuous Mesoproterozoic sources (94.3%), where the Stenian (1000–1200 Ma) interval comprises more than 50% of the zircon grains analysed. Neoproterozoic ages (897–996 Ma) are subordinate (3.4%). Famatinian (374–496 Ma) zircon ages represent 2.2% of the total.

In summary, the Talacasto Formation displays equally distributed ages of the Grenvillian-Sunsas, Pampean–Brazilian and Famatinian orogenic cycles (Fig. 16). The age of the youngest zircon is 397 ± 43 Ma, and the oldest is 2133 ± 21 Ma. The Punta Negra Formation instead, exhibits a major contribution from source rocks of the Grenvillian-Sunsas orogenic cycle. The age of the youngest zircon is 374 ± 2 Ma, whereas the oldest is 2588 ± 24 Ma. The two formations share a common Mesoproterozoic provenance, although the distribution of such source within the basin is uneven. Detrital contributions derived from Famatinian and Pampean–Brazilian source rocks are greater towards the north (Fig. 16).

Discussion

Following the classification of Folk et al. (1970), the rocks are sandstones (litharenites), as formerly established by Bustos (1995), instead of wackes as proposed by other authors (e.g., Loske 1994). Q-F-L diagram indicates a depositional basin linked to an orogen for the Gualilán Group, and the Qm-F-Lt diagram further shows an increase, towards younger ages, of the input of detritus derived from

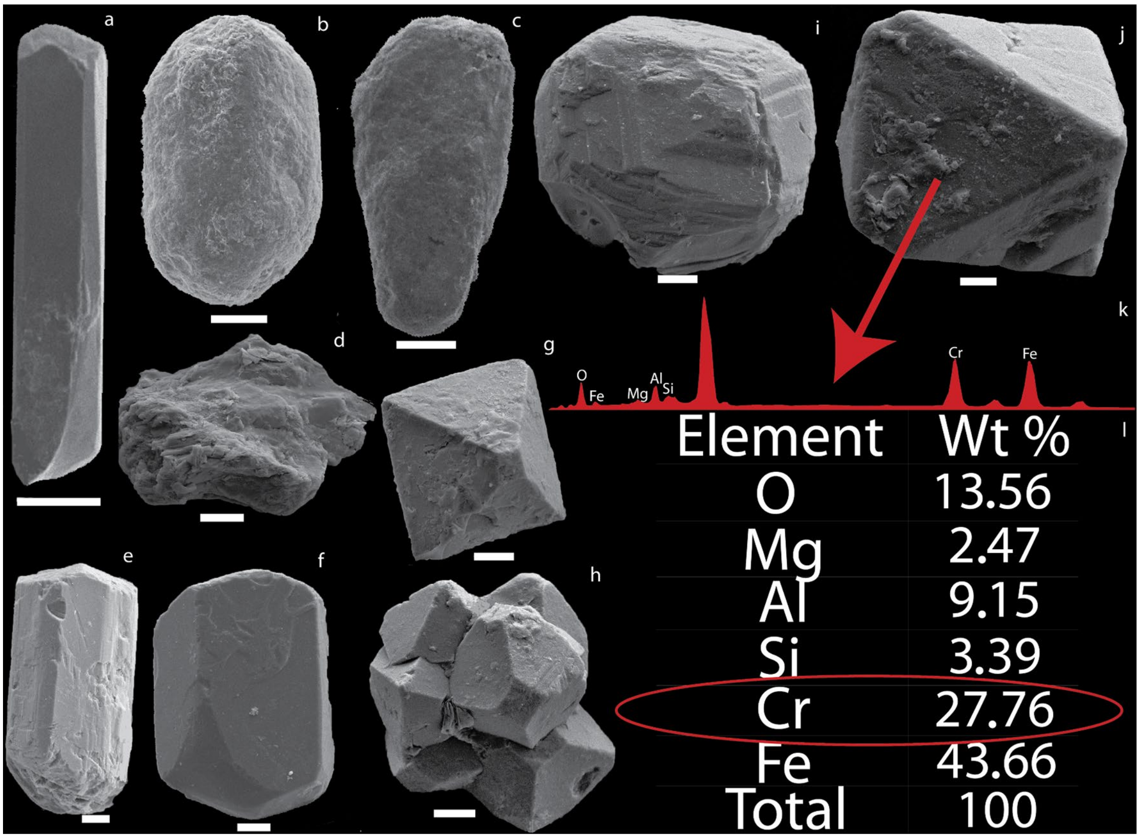

Fig. 8 Association of heavy minerals of the Gualilán Group. **a**, **b**, **c** Rutile. **d** Epidote. **e**, **f** Tourmaline. **g**, **h** Spinel. **i** Garnet. **j** Chromian Spinel. **k** Elements recognized by EDAX. **l** Semi-quantification of elements in EDAX. Scale bar = 100 μm

Unit		Group	Morphology	Families	Elongation (E)	Dimensions	Typology	Image
Devonian (Gualilán Group)	Punta Negra Formation	Group 1 Plutonic	Short prismatic crystals, bipyramidal faces and simple facets	F1	< 0.60-0.40	Width: 90.8 μm-120.3 μm Length: 156.1μm-200.3μm		
				F2	< 0.40-0.33	Width : 58.8μm-108.5μm Length: 166.6μm-210.6μm		
		Group 2 Metamorphic	Short prismatic crystals, multifaceted	F1	1- 0.67	Width : 102.5μm- 125.6μm Length: 126.9μm- 152.7μm		
				F2	<0.67-0.40	Width : 60.3μm- 101.5μm Length: 124.1μm- 158.4μm		
		Group 3 Recycled	Rounded crystals		≅ 1			
	Talacasto Formation	Group 1 Plutonic	Short prismatic crystals, bipyramidal faces and simple facets	F1	< 0.60-0.40	Width: 47.6 μm-50.1 μm Length: 78.9μm-121.4μm		
				F2	< 0.40-0.33	Width: 47.1 μm-52.3 μm Length:120.0μm-131.35μm		
		Group 2 Metamorphic	Short prismatic crystals, multifaceted	F1	<0.67-0.40	Width : 51.1μm- 55μm Length: 89.1μm - 116.2μm		
		Group 3 Recycled	Rounded crystals		≅ 1			

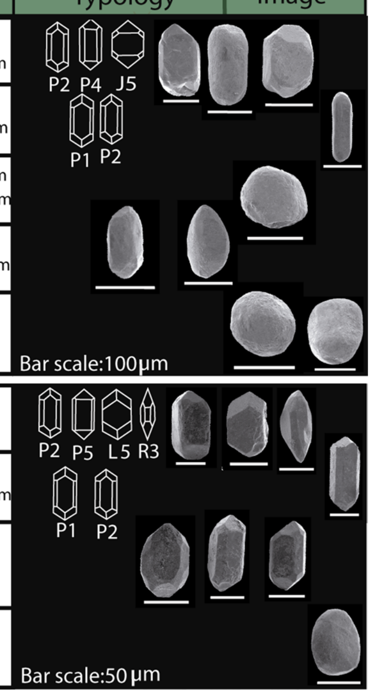

Fig. 9 Zircon morphology according to Gärtner et al. (2013); typology according to Pupin (1980) only for plutonic zircons

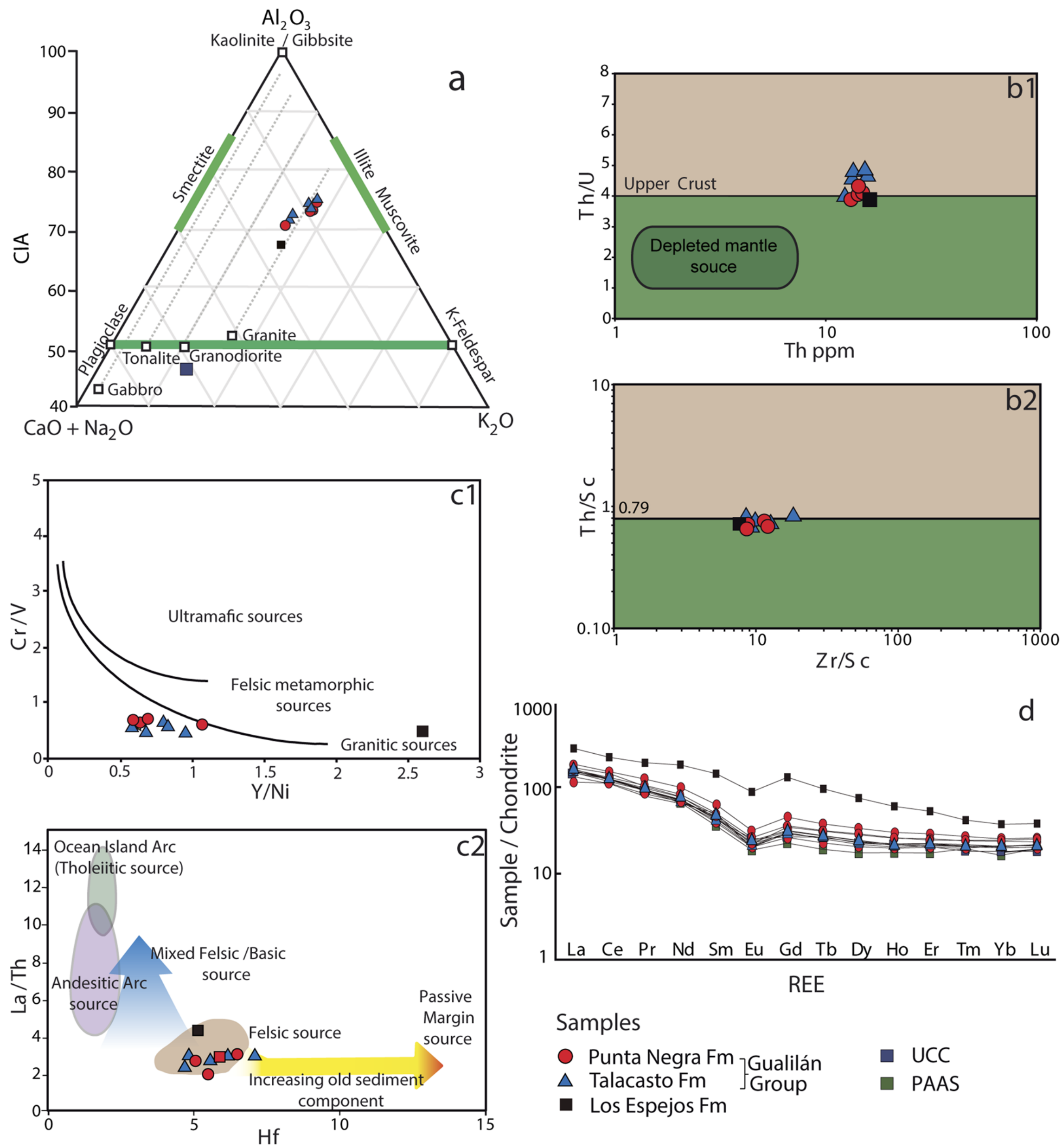

Fig. 10 **a** A-CN-K diagram for the Gualilán Group. Idealized mineral compositions and crystalline rocks values are according to Taylor and McLennan (1985). Dotted lines indicate the predicted weathering trend for the average parental rock compositions (Nesbitt and Young 1984, 1989). Note that the lower part of the diagram with A < 40 is not shown. The left side of the figure shows the range of CIA values. **b1** Th/U vs Th diagram (after McLennan et al. 1993). **b2** Th/Sc vs Zr/Sc diagram (after McLennan et al. 2003). **c1** Cr/V vs. Y/Ni diagram (after Hiscott 1984). Upper and lower curves represent the mixing lines of ultramafic (Cr/V = 45; Y/Ni = 0.001), felsic metamorphic (Cr/V = 1.23; Y/Ni = 1.02), and granitic (Cr/V = 0.25; Y/Ni = 2.33) rocks (Dinelli et al. 1999). **c2** La/Th vs. Hf diagram (after Floyd and Leveridge 1987). Fields indicate the compositions of sedimentary rocks deposited in different tectonic settings. Samples from the Gualilán Group plot into the field of felsic source. **d** Chondrite-normalized REE patterns from the Gualilán Group. PAAS: Post-Archean Australian Shales (Nance and Taylor 1976); UCC: upper continental crust (Rudnick and Gao 2003). Chondrite normalization values are from Sun and McDonough (1989). "Red coloured circle" Punta Negra Formation. "Blue coloured triangle" Talacasto Formation. "Black coloured square" Los Espejos Formation

Table 4 Selected element ratios of the Gualilán Group and Los Espejos Formation

Formation	Sample	Th/Sc	Zr/Sc	Cr/V	Y/Ni	La/Th	Th/U
Punta Negra	16PN34	0.72	8.87	0.69	0.59	2.83	4.33
	16PN44	0.68	12.14	0.72	0.69	3.07	3.94
	16PN52	0.68	8.77	0.67	0.63	1.91	4.14
	16PN58	0.75	11.36	0.61	1.06	3.25	4.06
Talacasto	16T08	0.83	8.58	0.50	0.94	2.44	4.65
	16T11	0.74	12.39	0.59	0.61	2.92	4.59
	16T38	0.68	8.97	0.60	0.82	2.96	4.86
	16T46	0.83	18.23	0.63	0.80	2.98	4.0
	16T65	0.76	9.86	0.48	0.68	2.77	4.87
Los Espejos	16LE29	0.69	7.90	0.47	2.55	4.49	3.95

Table 5 Rare Earth elements (expressed in ppm)

Formation	Sample	La	Ce	Pr	Nd	Sm	Eu	Gd	Tb	Dy	Ho	Er	Tm	Yb	Lu	ΣREE
Punta Negra	16PN34	40.4	80.2	9.33	33.5	6.11	1.19	5.48	0.86	5.25	1.13	3.38	0.51	3.62	0.54	191.50
	16PN44	39.9	83.2	10.44	40.2	7.87	1.54	7.52	1.20	7.49	1.50	4.10	0.63	4.21	0.65	210.45
	16PN52	28.4	71.4	8.30	32.9	7.30	1.29	7.25	1.18	7.26	1.48	4.27	0.62	4.08	0.60	176.33
	16PN58	46.2	97.4	12.32	48.4	9.98	1.86	9.55	1.44	8.66	1.73	4.88	0.70	4.37	0.67	248.16
Talacasto	16T08	38.5	77.3	9.09	32.9	6.45	1.23	6.05	0.99	6.02	1.23	3.57	0.54	3.55	0.56	187.98
	16T11	38.9	80.0	9.29	35.1	6.98	1.36	6.49	1.03	6.2	1.26	3.74	0.53	3.46	0.52	194.86
	16T38	40.2	80.3	9.66	37.3	7.51	1.42	6.64	1.05	6.28	1.24	3.75	0.54	3.61	0.54	200.04
	16T46	36.9	74.3	9.11	34.2	6.87	1.24	6.29	0.96	5.61	1.16	3.50	0.53	3.41	0.52	184.60
	16T65	41.9	92.8	10.16	37.6	6.97	1.31	6.02	0.99	5.97	1.28	3.74	0.56	3.57	0.56	213.43
Los Espejos	16LE29	71.0	143.5	19.22	89.3	23.05	5.34	28.12	3.73	19.68	3.52	9.01	1.09	6.49	0.99	424.04
	PAAS	38.0	80.0	8.90	32.0	5.60	1.10	4.70	0.77	4.40	1.0	2.90	0.50	2.80	0.50	183.17
	UCC	31.0	63.0	7.10	27.0	4.70	1.0	4.0	0.70	3.90	0.83	2.30	0.30	2.0	0.31	148.14

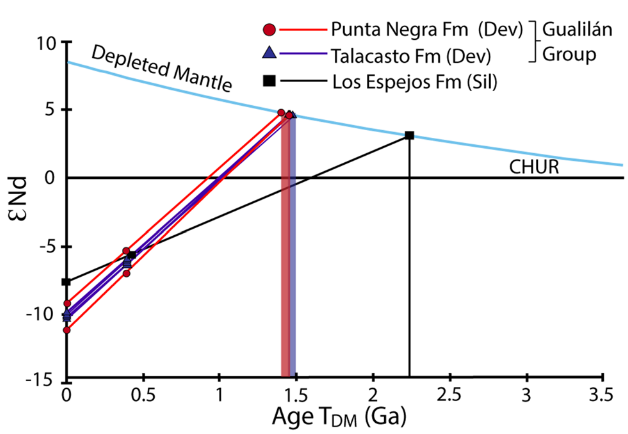

Fig. 11 ε_{Nd} vs. age. Samples were compared to *CHUR* (Chondritic Uniform Reservoir)

metamorphic sources. Heavy mineral assemblages of Devonian units of the Precordillera dominated by zircon, rutile and tourmaline indicate provenance from areas with mature rocks showing very low-grade metamorphism (Loske 1992, 1994). However, rutile and tourmaline derived from high-grade metamorphic rocks are known in several regions (e.g., Mange and Maurer 1992; Konzett et al. 2012; Broska and Petrík 2015). Furthermore, Loske (1992) recognized the same low diverse heavy mineral assemblage throughout the Cambrian to Silurian units of the Precordillera. More recently, other minerals were recognized in Ordovician to Silurian units of the Cuyania terrane (Pavón, Don Braulio and Ponón Trehué formations), such as chromium spinel and apatite (Abre et al. 2009, 2011).

The heavy mineral assemblage of the Devonian Gualilán Group comprises garnet, staurolite, apatite, epidote, monazite, and titanite, indicating that high-grade metamorphic and igneous rocks were exhumed and exposed to erosion. Chromium-rich spinel of the Talacasto Formation (Fig. 8) derived from mafic rocks probably located at the Pie de Palo Range. Morphological studies of detrital zircon following Pupin (1980) and Gärtner et al. (2013) give a broad estimation regarding the nature of the felsic source rocks. Within the Gualilán Group, prevail the zircon grains originally crystallized in a plutonic environment which underwent posterior metamorphism before deposition within the Gualilán Group, followed in order of abundance by those crystallized

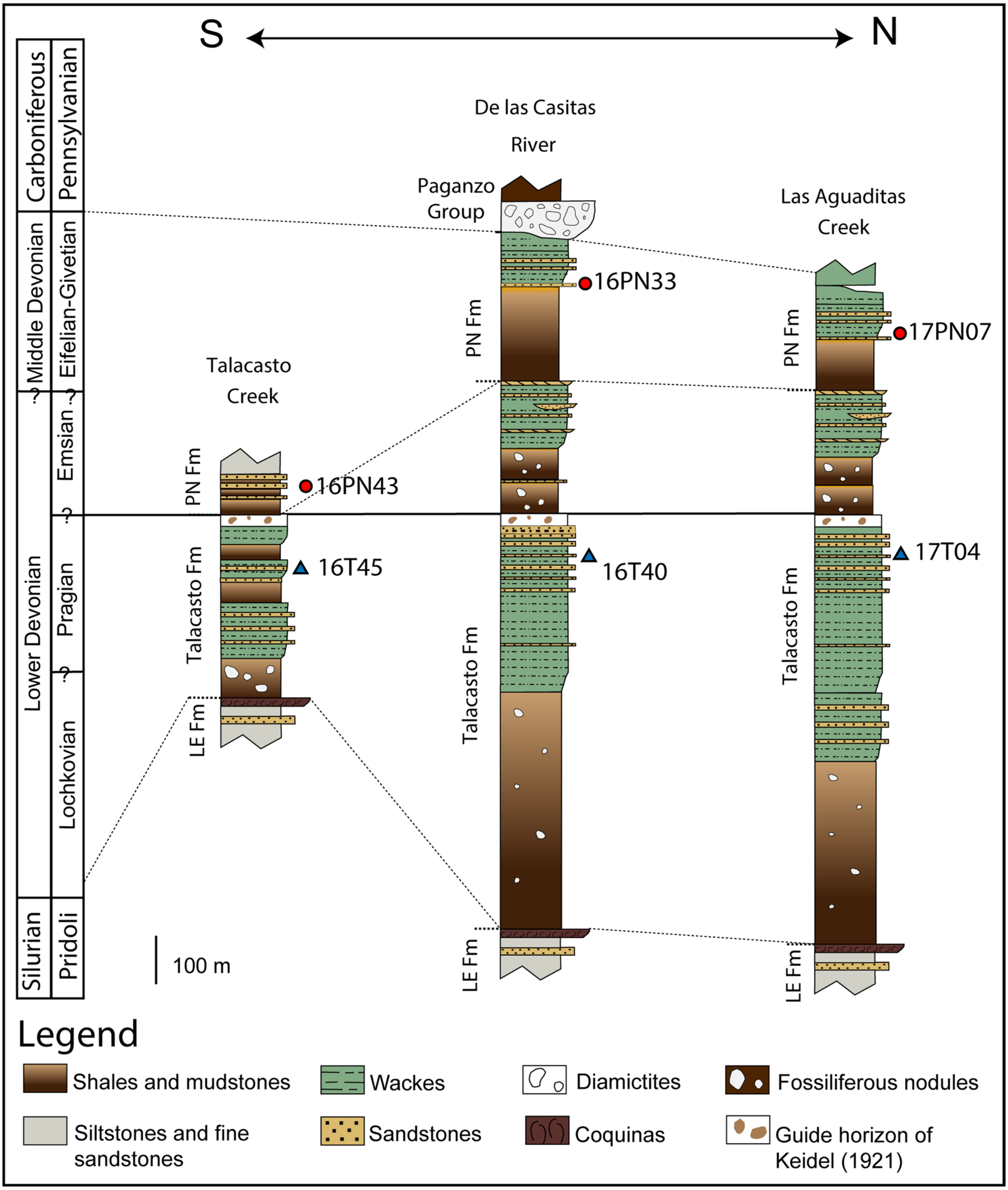

Fig. 12 Stratigraphic columns showing the different studied sections with location of the samples analysed by U–Pb geochronology. *PN Fm* Punta Negra Formation, *LE Fm* Los Espejos Formation

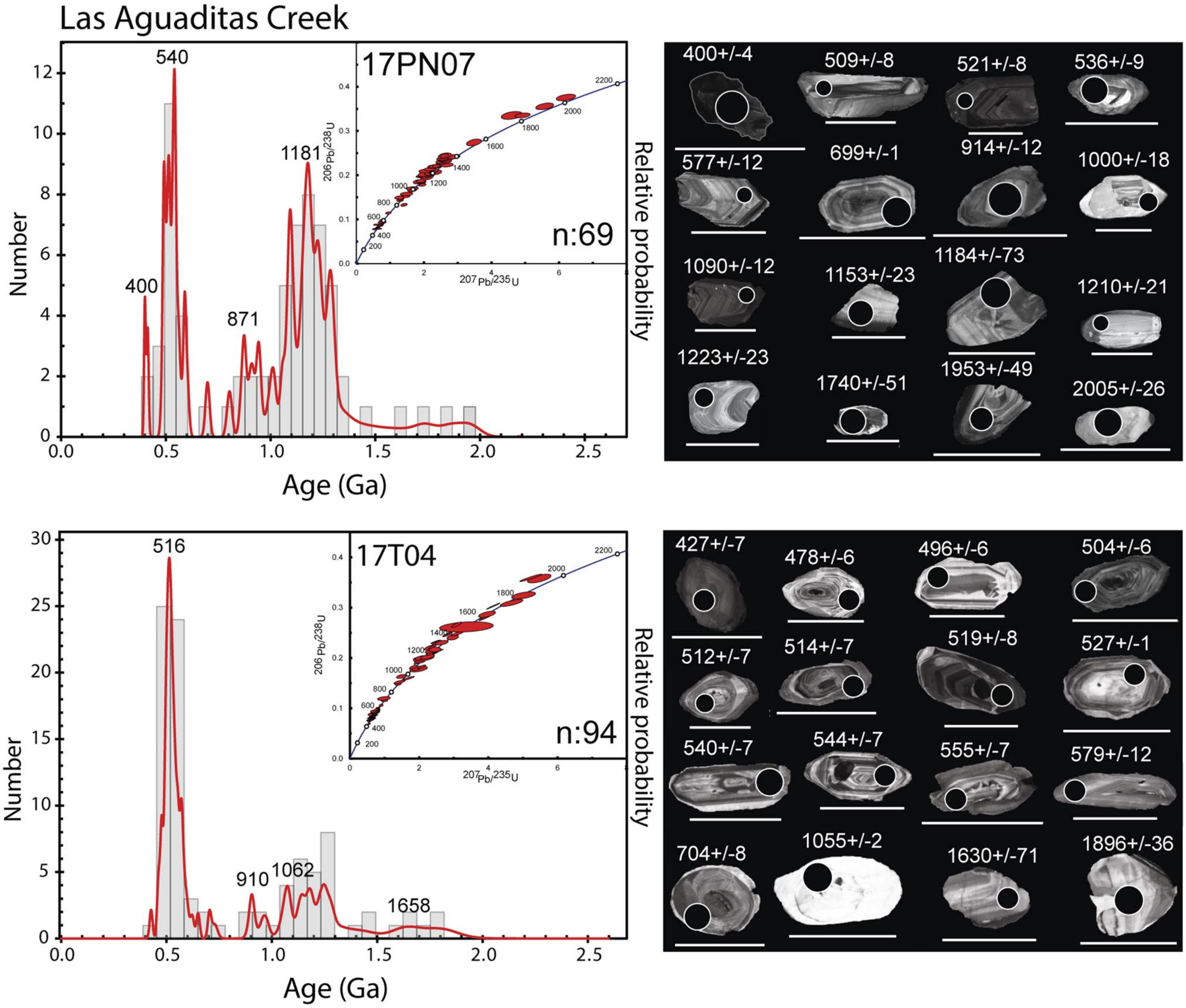

Fig. 13 Frequency histograms and probability curves of detrital zircon ages from the sampled levels of the Gualilán Group in the Las Aguaditas Creek. Lower: (17T40) Talacasto Formation, Upper: (17PN07) Punta Negra Formation, with Concordia diagrams. Right: cathodoluminescence images of selected zircon grains. Scale bar = 100 µm; ages and errors in Ma

in plutonic environments. This is in agreement with Th/U ratios indicative of plutonic sources. Geochemical provenance proxies support derivation from a felsic provenance component that underwent moderate weathering and very scarce reworking.

The narrow range of negative ε_{Nd} values of the Gualilán Group points to restricted variation in the detrital mix of crustal sources. Nd data from the Umango, Maz and Pie de Palo ranges, and the San Rafael and Las Matras blocks show ε_{Nd} values in the range of variation of data calculated to the time of deposition of the Gualilán Group (Sato et al. 2004; Cingolani et al. 2005; Vujovich et al. 2005; Rapela et al. 2010; Varela et al. 2011). The T_{DM} ages of the Gualilán Group in between 1.4 and 1.5 Ga are comparable to T_{DM} ages for Mesoproterozoic basement rocks of the Cuyania terrane (Kay et al. 1996; Sato et al. 2004; Vujovich et al. 2005; Rapela et al. 2010; Varela et al. 2011).

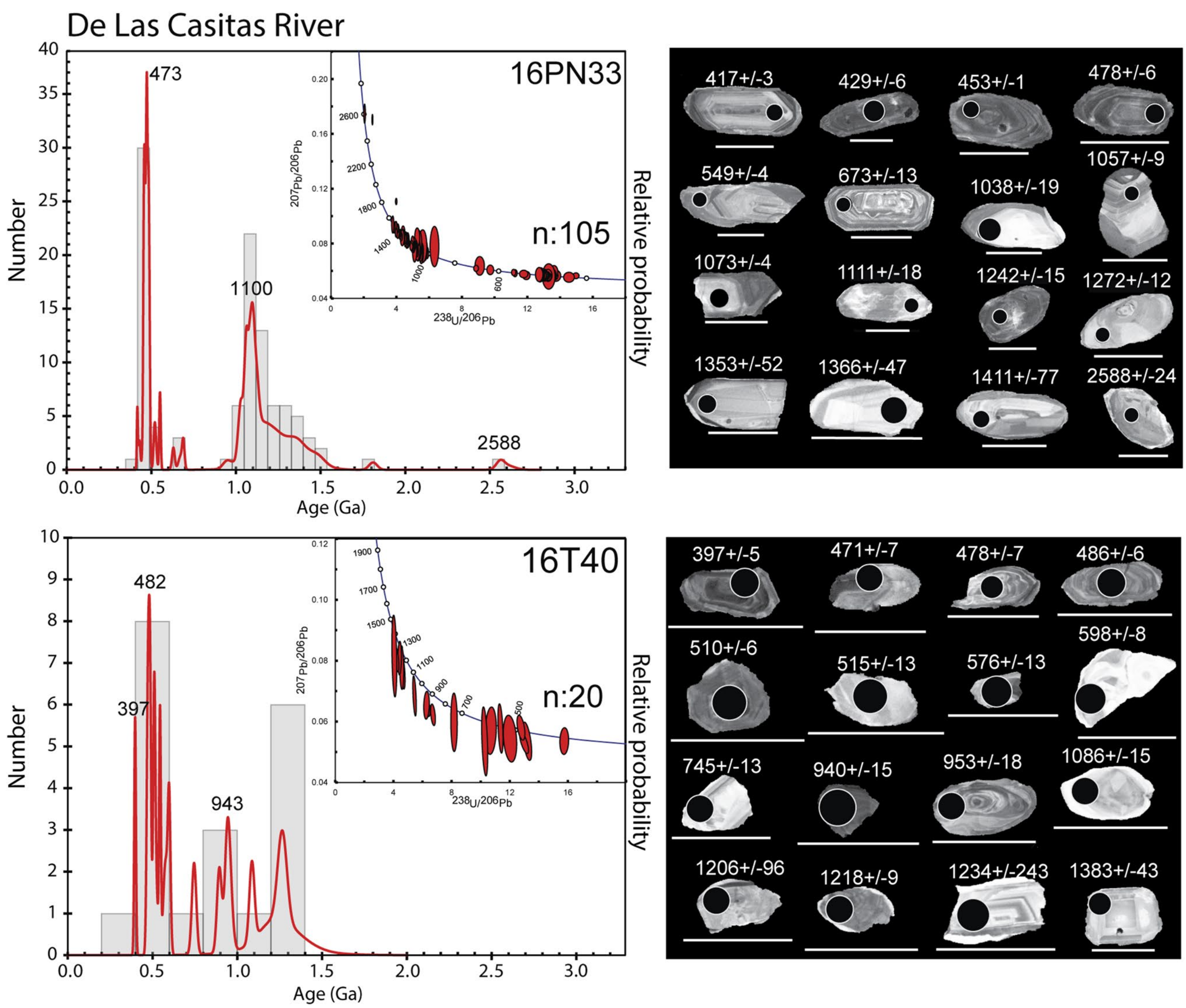

Fig. 14 Frequency histograms and probability curves of detrital zircon ages from the sampled levels of the Gualilán Group in the Las Casitas River. Lower: (16T40) Talacasto Formation, Upper: (16PN33) Punta Negra Formation, with Tera-Wasserburg diagrams. Right: cathodoluminescence images of selected zircon grains. Scale bar = 100 µm; ages and errors in Ma

The detrital zircon ages of the Talacasto Formation reveal a provenance from rocks formed during two orogenic cycles: Pampean–Brazilian and Grenvillian-Sunsas. Outcrops of these rocks are presently located eastwards of the Gualilán basin, at the so-called eastern and western Pampean Ranges, respectively. Famatinian detrital zircon ages are more abundant towards the north of the basin (at Las Aguaditas Creek and de las Casitas River). The main zircon population of the Punta Negra Formation is Mesoproterozoic in age (1000–1200 Ma). Grenvillian-aged rocks that could account for this provenance are found in the western Pampean Ranges (Pie de Palo, Umango, Espinal and Maz ranges). The oldest ages corresponding also to the Grenvillian-Sunsas orogenic cycle could have been derived from the

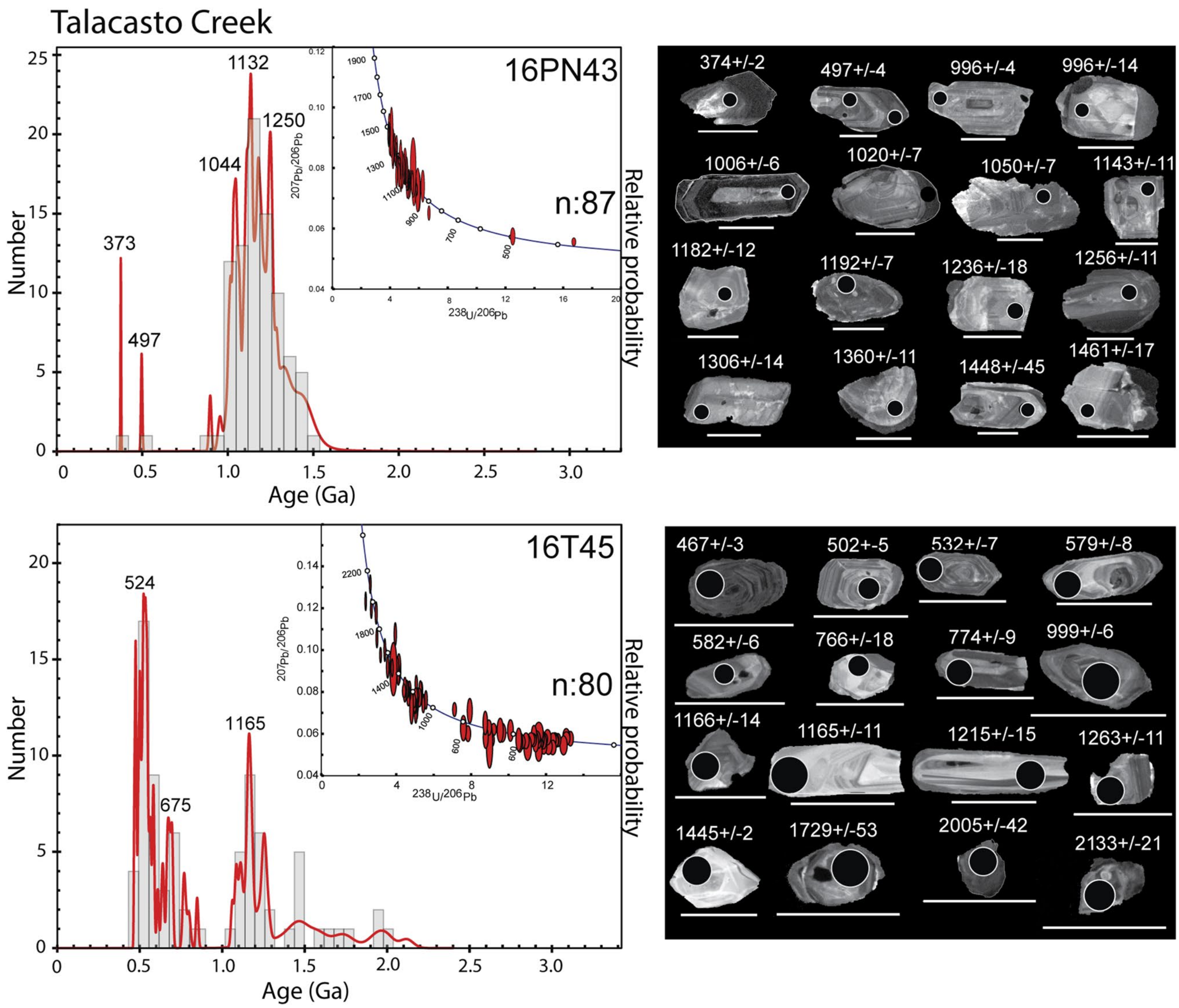

Fig. 15 Frequency histograms and probability curves of detrital zircon ages from the sampled levels of the Gualilán Group in the Talacasto Creek. Lower: (16T45) Talacasto Formation, Upper: (16PN43) Punta Negra Formation, with Tera-Wasserburg diagrams. Right: cathodoluminescence images of selected zircon grains. Scale bar = 100 μm; ages and errors in Ma

Maz-Umango Complexes located to the east of the Gualilán basin (Mingramm 1985; Galindo et al. 2004; Rapela et al. 2010; Varela et al. 2011; Ramacciotti et al. 2015).

The visual comparison of the U–Pb probability distribution diagrams (Fig. 17a), can be enhanced by statistical analysis. The Kolmogorov–Smirnov (K–S) two-sample test was applied to assess the heterogeneity of the age distributions (Berry et al. 2001; Fig. 17a; Table 6). This test provides a means to mathematically compare two detrital zircon age distributions to determine if there is a statistically significant difference between them. The method is independent of any assumptions about the probability distribution of a sample and allows comparison of both, age values (peak locations) and distributions (peak shapes), using the P-parameter (DeGraaff-Surpless et al. 2003).

Samples of the Gualilán Group show a good correlation between each other (Table 6), except for sample 16PN43, that displays a P value of 0 with respect to all

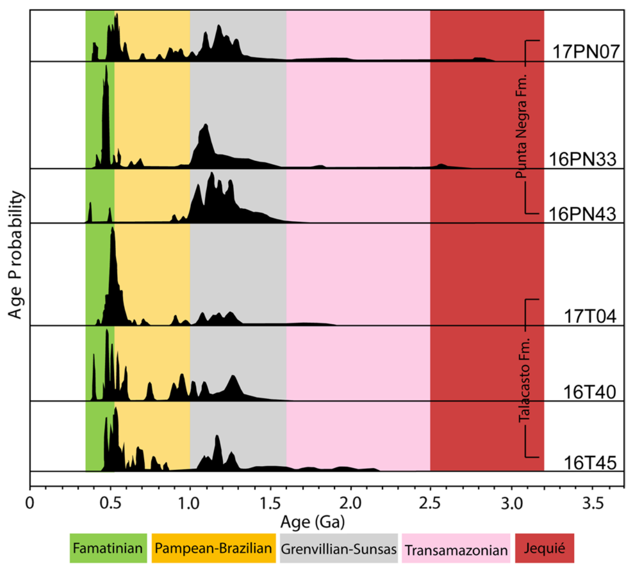

Fig. 16 Overview of the main detrital zircon populations found in the Gualilán Group, indicating that three main sources are responsible for the vast majority of the observed ages. The probability density distribution diagram for each sample is shown. Different colours are from recognized South American orogenic cycles: Jequié (Archean) to Transamazonian (Paleoproterozoic), Grenvillian-Sunsas (Mesoproterozoic), Pampean–Brazilian (Neoproterozoic–Early Cambrian) and Famatinian (Middle/Late Cambrian-Devonian)

other samples analysed. This disparity is due to a domain of almost 95% of Mesoproterozoic ages (Fig. 17a).

Analogous methodologies to those used in the present work were applied to Devonian successions of the Cuyania terrane by several authors. The comparison with our data comes in handy to give further insights into the paleogeography of the SW margin of Gondwana. One of those successions is the Villavicencio Formation, cropping out in the Mendoza province, showing more than 70% of Mesoproterozoic detrital zircon ages followed by Pampean–Brazilian ages (Cingolani et al. 2013). Detrital zircon patterns of the Villavicencio and Punta Negra formations are very similar, pointing to comparable sources for both units (Fig. 17b). Another Devonian succession is the Río Seco de los Castaños Formation, exposed in the San Rafael Block which comprises prominent populations of Pampean–Brazilian and Famatinian detrital zircon ages (Cingolani et al. 2017), being different to all studied samples of the Gualilán Group. The sedimentary rocks of the Gualilán Group and Villavicencio Formation were deposited in a post-collisional setting, whereas the Río Seco de los Castaños Formation was deposited in a convergent setting, probably in an isolated depocentre (Fig. 17b).

Deposition of the Gualilán Group occurred within a peripheral foreland basin developed as a result of the post-collision of Cuyania against the SW margin of Gondwana.

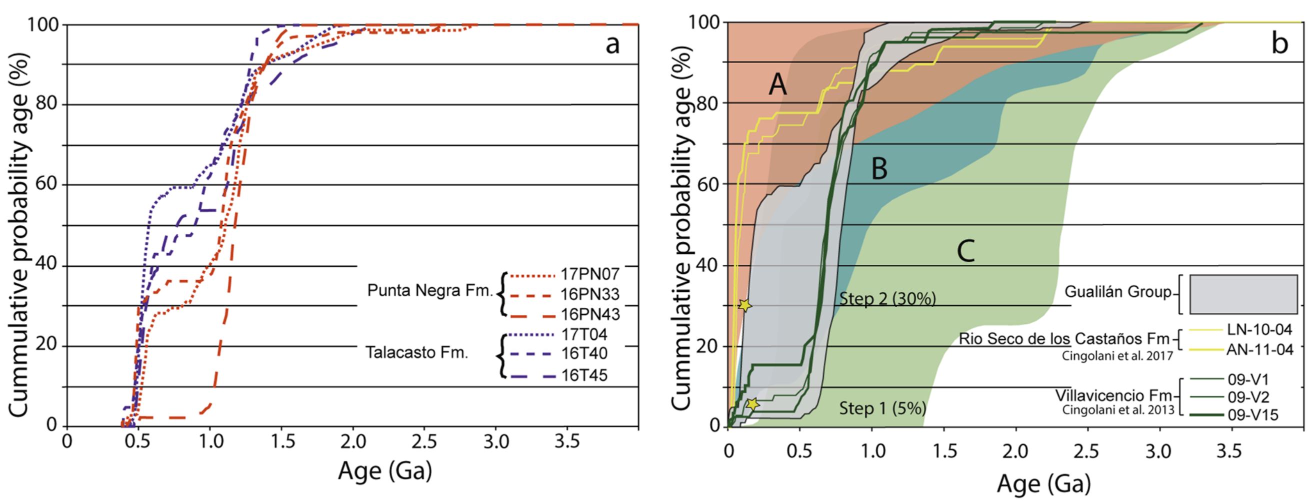

Fig. 17 a Kolmogorov–Smirnov (K–S) sample test. **b** Tectonic discrimination diagram after Cawood et al. (2012). Fields: **a** convergent, **b** collisional, **c** extensional

Table 6 Results of Kolmogorov–Smirnov test (with error CDF) for all samples analysed

	Sample	17T04	17PN07	16T40	16PN33	16T45	16PN43
KS *P* values using error in the CDF	17T04		0.001	*0.784*	0.001	*0.156*	0.000
	17PN07	0.001		*0.266*	0.024	0.049	0.000
	16T40	*0.784*	0.266		*0.185*	*0.843*	0.000
	16PN33	0.001	0.024	*0.185*		0.040	0.000
	16T45	*0.156*	0.049	*0.843*	0.040		0.000
	16PN43	0.000	0.000	0.000	0.000	0.000	
D values using error in the CDF	17T04		0.300	0.158	0.272	0.172	0.596
	17PN07	0.300		0.249	0.228	0.222	0.348
	16T40	0.158	0.249		0.261	0.151	0.574
	16PN33	0.272	0.228	0.261		0.207	0.338
	16T45	0.172	0.222	0.151	0.207		0.513
	16PN43	0.596	0.348	0.574	0.338	0.513	

[a] *P* values. "Blank indicates" $P < 0.05$; "italics indicates" $P > 0.05$

[b] *D* values

The bulk of the detritus derived from plutonic and metamorphic felsic rocks with compositions and isotopic signatures pointing to Famatinian, Pampean–Brazilian and Grenvillian-Sunsas aged rocks. During the Early Devonian, the Talacasto Formation received an input from both, the eastern and western Pampean Ranges. The uplift of the Western Pampeanas Ranges before deposition of the Middle Devonian Punta Negra Formation explains the restriction to Mesoproterozoic sources within its sedimentary record (Fig. 18).

Final remarks

- Petrographical and geochemical data show that both units studied of the Gualilán Group underwent moderate weathering and point to an average source composition similar to UCC, or slightly more felsic. Both Devonian successions were fed by igneous and metamorphic sources, as demonstrated by lithoclast types, heavy mineral assemblages and detrital zircon morphological families. The presence of chromium-rich mineral grains (likely chromium spinel) in the so-called 'Keidel's guide level', found within the Talacasto Formation, evidence that a mafic source provided detritus during Pragian-Emsian times.
- Sm–Nd isotope data and particularly U–Pb detrital zircon data indicate a contribution from felsic crustal rocks of Famatinian, Pampean–Brazilian and Grenvillian-Sunsas aged sources for the Talacasto Formation, whereas the bulk of the detritus derived mostly from Mesoproterozoic sources for the Punta Negra Formation. The scarce contributions of Archean and Paleoproterozoic sources indicate that the Río de la Plata Craton was not an important source for the Devonian basin.
- Probable source rocks are located towards the east of the peripheral foreland Gualilán basin, within the eastern and western Pampean Ranges. In the context of the paleogeography of SW Gondwana, these provenance patterns indicate high exhumation and erosion rates of the Grenvillian Orogen for Devonian time and, on the contrary, a low exhumation/erosion rate of the cratonic areas during the Middle Devonian.

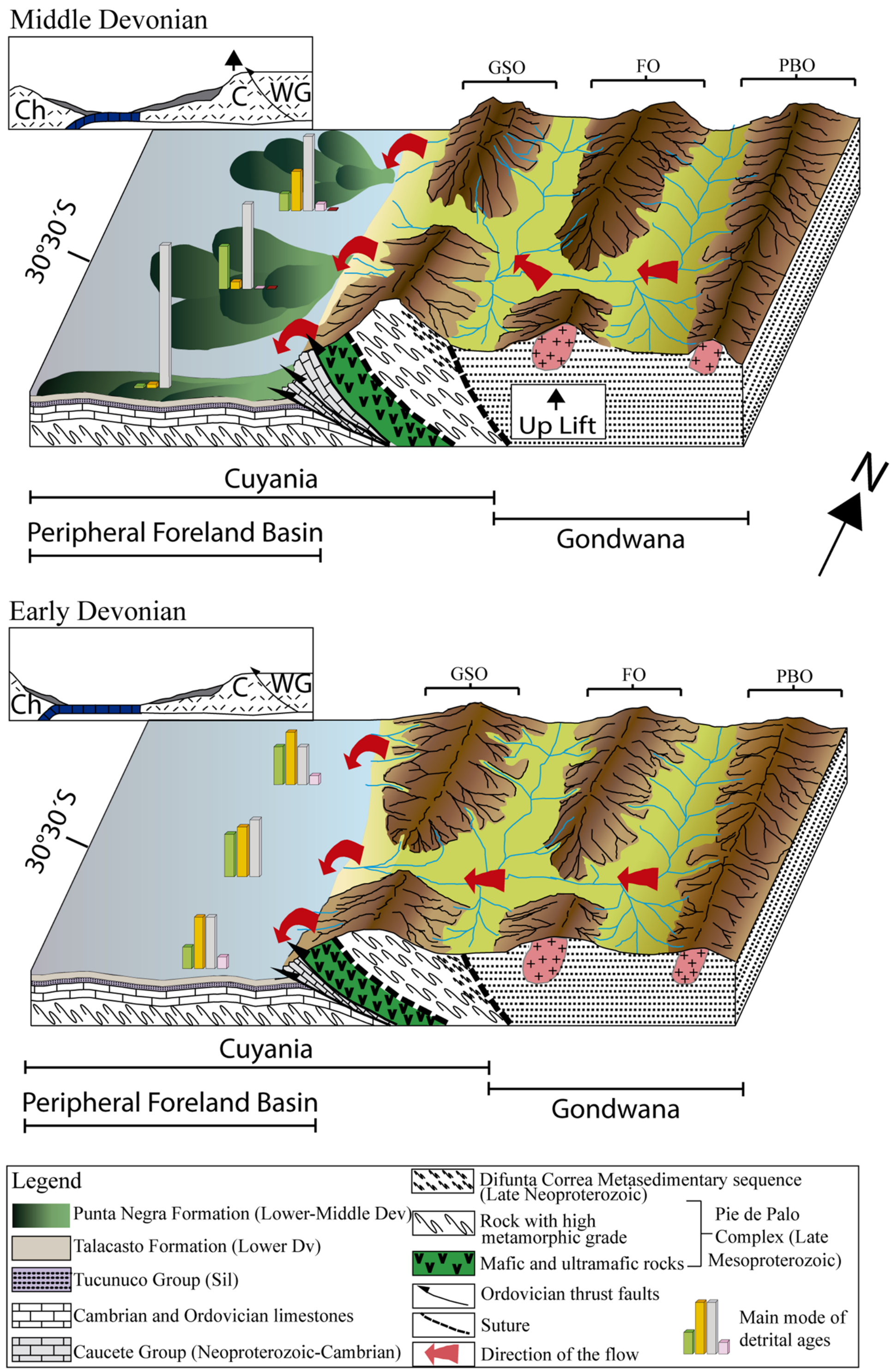

Fig. 18 Block diagram showing the Devonian distribution for the Gualilán Group, a peripheral foreland basin located westwards of the western margin of Gondwana developed in the vicinity of the Grenvillian-Sunsas orogen which is the most likely source of detritus. The highlands located in the East comprise the Grenvillian-Sunsas (GSO), Pampean–Brazilian (PBO) and Famatinian (FO) orogens. The colours of the histograms are related to the orogenic cycle from which the detrital zircon derived (see Fig. 16), whereas the height is proportional to the percentage of each of them. *Ch* Chilenia Terrane, *C* Cuyania Terrane, *WG* Western Gondwana. Top left insets show the subduction between western Gondwana (with Cuyania already accreted) and Chilenia terrane

Acknowledgements This research was partially financed by CONICET (Grant PUE-CIG). The Centro de Investigaciones Geológicas (CIG, La Plata, Argentina) provide the laboratory facilities for sample preparations. We wish to especially thank W. Loske (Germany) for his very relevant comments. Appreciation is extended to CPGeo and technical staff of the University of Sao Paulo, Brazil. To Dr Silvio Peralta from San Juan University, for helped and guided us during field trips along the Central Precordillera. To Dr Víctor A. Ramos from the University of Buenos Aires for his helpful comments. Contribution to Project PPID/N031 (2018–2020), La Plata University. The careful and insightful reviews of Guido Meinhold, Mauricio Calderón and the comments of the journal editor have benefited this article and are gratefully acknowledged.

References

Abre P, Cingolani C, Zimmermann U, Cairncross B (2009) Detrital chromian spinels from upper Ordovician deposits in the Precordillera terrane, Argentina: a mafic crust input. J S Am Earth Sci 28(4):407–418

Abre P, Cingolani C, Zimmermann U, Cairncross B, Chemale F Jr (2011) Provenance of Ordovician clastic sequences of the San Rafael block (central Argentina), with emphasis on the Ponón Trehué Formation. Gondwana Res 19(1):275–290

Aceñolaza FG, Miller H, Toselli AJ (2002) Proterozoic-early paleozoic evolution in western South America—a discussion. Tectonophysics 354(1–2):121–137

Amos AJ, Boucot AJ (1963) A revision of the brachiopod family Leptocoelidae. Palaeontology 6:440–457

Arnol JA, Coturel EP (2017) Plantas de la Formación Punta Negra (Devónico) en la Precordillera de San Juan, Argentina. Reunión de comunicaciones de la Asociación Paleontológica Argentina. San Luis, Argentina. Libro de resúmenes 11

Astini RA (1990) Cuerpos de arenas en la Formación Talacasto. Plataforma fangosa del Devónico Precordillerano, Provincia de San Juan. Tercera reunión Argentina Sedimentología. San Juan, pp 13–18

Astini RA (1991a) Paleoambientes sedimenterios y secuencias depositacionales del Ordovícico clástico de la Precordillera Argentina. Tesis Doctoral. Universidad Nacional de Córdoba, 851 pp (Unpublished)

Astini RA (1991b) Sedimentología de la Formación Talacasto: plataforma fangosa del Devónico precordillerano, provincia de San Juan. Rev Asoc Geol Argent 44:277–294

Astini RA (1992) Tectofacies ordovícicas y evolución de la cuenca eopaleozoica de la Precordillera Argentina. Estud Geol 48(5–6):315–327

Astini RA (1996) Las Fases Diastróicas del Paleozoico medio en la Precordillera del Oeste Argentino -Evidencias Estratigráicas. XIII Congreso Geológico Argentino y III Congreso de Exploración de Hidrocarburos, Actas V, pp 509–526. Buenos Aires

Astini RA, Maretto HM (1996) Análisis estratigráico del Silúrico de la Precordillera Central de San Juan y consideraciones sobre la evolución de la cuenca. XIII Congreso Geológico Argentino, pp 351–368

Baldis BA (1975) El Devónico Inferior en la Precordillera Central, Parte I: Estratigrafía: Revista de la Asociación Geológica Argent 30:53–83

Baldis BA, Rossi de García E (1972) Ostracodes devonniens argentins associés a l´faune Malvinokafrique Veme Congrés Africain de Micro-paléontologie (Addis Abeba), pp 57–92

Basilici G, de Luca PHV, Poiré DG (2012) Hummocky cross-stratification-like structures and combined-flow ripples in the Punta Negra Formation (Lower-Middle Devonian, Argentine Precordillera): a turbiditic deep-water or storm-dominated prodelta inner-shelf system? Sediment Geol 267:73–92

Berry RF, Jenner GA, Meffre S, Tubrett MN (2001) A North American provenance for Neoproterozoic to Cambrian sandstones in Tasmania? Earth Planet Sci Lett 192(2):207–222

Borrello AV (1969) Los geosinclinales de la Argentina. Dirección Nacional de Geología y Minería, Anales 14: 188. Buenos Aires

Bracaccini OI (1949) El perfil de Tambolar. Rev Asoc Geol Argent 4:165–179

Broska I, Petrík I (2015) Variscan thrusting in I-and S-type granitic rocks of the Tribeč Mountains, Western Carpathians (Slovakia): evidence from mineral compositions and monazite dating. Geol Carpath 66(6):455–471

Bustos UD (1995) Sedimentologia y evolucion paleoambiental de la Formacion Punta Negra en el sector central de la Precordillera de San Juan. Trabajo Final, Facultad de Ciencias Exactas, Fisicas y Naturales, Universidad Nacional de Cordoba, 120 pp (Unpublished)

Bustos UD (1996) Modelo sedimentario alternativo para el Devónico de la Precordillera central sanjuanina: formación Punta Negra. Rev Asoc Argent Sedimentol 3:17–30

Bustos UD, Astini RA (1997) Formación Punta Negra: Análisis secuencial y evolución de la Cuenca Devónica Precordillerana. Rev Asoc Argent Sedimentol 4:97–111

Carrera MG, Rustán JJ (2015) The new genus Talacastospongia: insights on the first record of a Devonian sponge from South America. J Paleontol 89(6):912–919

Cawood PA, Hawkesworth CJ, Dhuime B (2012) Detrital zircon record and tectonic setting. Geology 40(10):875–878

Cingolani CA, Ramos VA (2017) Pre-carboniferous tectonic evolution of the San Rafael block, Mendoza Province. In: Cingolani CA (ed) Pre-carboniferous evolution of the San Rafael block, Argentina, Chapter 13. Springer earth system sciences, pp 239–256. ISBN 978-3-319-50153-6

Cingolani CA, Llambias EJ, Basei MAS, Varela R, Chemale Junior F, Abre P (2005) Greenvillian and Famatinian-age ingneous events in the San Rafael block, Mendoza Province, Argentina: geochemical and isotopic constraints. Gondwana 12, p 250

Cingolani CA, Manassero MJ, Basei MAS, Uriz NJ (2013) Provenance of the Villavicencio Fm, Lower Devonian, Mendoza, Argentina. VII Congreso Uruguayo de Geología, Montevideo. Sociedad Geológica del Uruguay, Actas, pp 191–196

Cingolani CA, Uriz NJ, Abre P, Manassero MJ, Basei Mas (2017) Silurian-devonian land-sea interaction within the San Rafael Block, Argentina: Provenance of the Rio Seco de los Castanos Formation. In: Cingolani CA (ed) Pre-Carboniferous evolution of the San Rafael Block, Argentina, Chapter 10. Implications in the SW Gondwana margin. Springer, pp 183–208. ISBN 978-3-319-50153-6

Coturel E, Arnol J (2018) Plant remains from the Devonian of San Juan, Argentina. In: 5th International Paleontological Congress, Paris, France, p 818

Cuerda AJ, Baldis BA (1971) Silúrico-Devónico de la Argentina. Ameghiniana 8:128–164

Cullers RL (1995) The controls on the major-and trace-element evolution of shales, siltstones and sandstones of Ordovician to Tertiary age in the Wet Mountains region, Colorado, USA. Chem Geol 123(1–4):107–131

Dalla Salda L, Cingolani CA, Varela R (1992) Early Paleozoic orogenic belt of the Andes in southwestern. Geology 20:617–620

Davis JS, Roeske SM, McClelland WC, Snee LW (1999) Closing the ocean between the Precordillera terrane and Chilenia: early Devonian ophiolite emplacement and deformation in the southwest Precordillera. Special Papers-Geological Society of America, pp 115–138

DeGraaff-Surpless K, Mahoeney B, Wooden J, McWilliams M (2003) Lithofacies control in detrital zircon provenance studies: insights from the Cretaceous Methow Basin, southern Canadian Cordillera. Geol Soc Am Bull 115:899–915

DePaolo DJ (1981) Neodymium isotopes in the Colorado Front Range and crust–mantle evolution in the Proterozoic. Nature 291(5812):193

Dickinson WR, Gehrels GE (2003) U-Pb ages of detrital zircons from Permian and Jurassic eolian sandstones of the Colorado Plateau, USA: paleogeographic implications. Sediment Geol 163(1–2):29–66

Dickinson WR, Beard LS, Brakenridge GR, Erjavec JL, Ferguson RC, Inman KF, Ryberg PT (1983) Provenance of North American Phanerozoic sandstones in relation to tectonic setting. Geol Soc Am Bull 94(2):222–235

Dinelli E, Lucchini F, Mordenti A, Paganelli L (1999) Geochemistry of Oligocene-Miocene sandstones of the northern Apennines (Italy) and evolution of chemical features in relation to provenance changes. Sediment Geol 127(3–4):193–207

Edwards D, Morel E, Poiré DG, Cingolani CA (2001) Land plants in the Devonian Villavicencio Formation, Mendoza Province. Argent Rev Palaeobot Palynol 116(1–2):1–18

Edwards D, Poiré DG, Morel EM, Cingolani CA (2009) Plant assemblages from SW Gondwana: further evidence for high-latitude vegetation in the Devonian of Argentina. Geol Soc London Spec Publ 325(1):233–255

Fedo CM, Nesbitt HW, Young GM (1995) Unraveling the effects of potassium metasomatism in the sedimentary rocks and paleosols with implications for paleoweathering conditions and provenance. Geology 23:921–924

Fedo CM, Sircombe KN, Rainbird RH (2003) Detrital zircon analysis of the sedimentary record. Rev Mineral Geochem 53(1):277–303

Finney S, Gleason J, Gehrels G, Peralta S, Aceñolaza G (2003) Early Gondwanan connection for the Argentine Precordillera terrane. Earth Planet Sci Lett 205(3–4):349–359

Floyd P, Leveridge B (1987) Tectonic environment of the Devonian Gramscatho basin, south Cornwall: framework mode and geochemical evidence from turbiditic sandstones. J Geol Soc London 144:531–542

Folk RL, Andrews PB, Lewis D (1970) Detrital sedimentary rock classification and nomenclature for use in New Zealand. N Z J Geol Geophys 13(4):937–968

Galindo C, Casquet C, Rapela C, Pankhurst RJ, Baldo E, Saavedra J (2004) Sr, C and O isotope geochemistry and stratigraphy of Precambrian and lower Paleozoic carbonate sequences from the Western Sierras Pampeanas of Argentina: tectonic implications. Precambr Res 131(1–2):55–71

Gärtner A, Linnemann U, Sagawe A, Hofmann M, Ullrich B, Kleber A (2013) Morphology of zircon crystal grains in sediments- characteristics, classifications, definitions. Geol Saxonica 59:65–73

Goldstein SL, Arndt NT, Stallard RF (1997) The history of a continent from U-Pb ages of zircons from Orinoco River sand and Sm-Nd isotopes in Orinoco basin river sediments. Chem Geol 139(1–4):271–286

González Bonorino G (1975) Sedimentología de la Formación Punta Negra y algunas consideraciones sobre la geología regional de la Precordillera de San Juan y Mendoza. Rev Asoc Geol Argent 30:223–246

González Bonorino G, Middleton GN (1976) A Devonian submarine fan in western. Argent J Sediment Petrol 46:56–69

Heredia N, Farias P, García-Sansegundo J, Giambiagi L (2012) The basement of the Andean Frontal Cordillera in the Cordón del Plata (Mendoza, Argentina): geodynamic evolution. Andean Geol 39(2):242–257

Heredia N, García-Sansegundo J, Gallastegui G, Farias P, Giacosa RE, Giambiagi LB, Rubio-Ordóñez Á (2018) Review of the geodynamic evolution of the SW margin of Gondwana preserved in the Central Andes of Argentina and Chile (28°-38° S latitude). J S Am Earth Sci 87:87–94

Herrera ZA (1993) Nueva precisiones sobre la edad de la Formación Talacasto (Precordillera Argentina) en base a su fauna de braquiópodos. XII Congreso Argentino y II Congreso de Exploración de Hidrocarburos, Buenos Aires, pp 289–295

Herrera ZA (1995a) The first notanopliid brachiopod from the South American Devonian sequence. Geobios 28:337–342

Herrera ZA (1995b) The Lower Devonian chonetoidean brachiopods from Argentine Precordillera. In: Racheboeuf P (ed) Four contributions to the study of chonetoidean brachiopods, vol 136. Centre des Sciences de la Terre, Université Claude-Bernard-Lyon I, Lyon, pp 101–147

Herrera ZA, Bustos UD (2001) Braquiópodos devónicos de la Formación Punta Negra, en el perfil del Río de las Chacritas. Precordillera Argent Ameghiniana 38(4):367–374

Hiscott R (1984) Ophiolitic source rocks for Taconic-age flysch: trace-element evidence. Geol Soc Am 95:1261–1267

Ingersoll RV, Bullard TF, Ford RL, Grimm JP, Pickle JD, Sares SW (1984) The effect of grain size on detrital modes: a test of the Gazzi-Dickinson point-counting method. J Sediment Res 54(1):103–116

Kay SM, Orrell S, Abbruzzi JM (1996) Zircon and whole rock Nd-Pb isotopic evidence for a Grenville age and a Laurentian origin for the basement of the Precordillera in Argentina. J Geol 104(6):637–648

Keidel J (1921) Observaciones geologícas en la Precordillera de San Juan y Mendoza. Anal Minist Agric Secc Geol Mineral Miner 15:7–102

Keller M (1999) Argentine Precodillera. Sedimentary and plate tectonic history of a Laurentian Crustal fragment in South America. Geo Soc Am Spec Paper 341:131

Konzett J, Rhede D, Frost DJ (2012) The high PT stability of apatite and Cl partitioning between apatite and hydrous potassic phases in peridotite: an experimental study to 19 GPa with implications for the transport of P, Cl and K in the upper mantle. Contrib Miner Petrol 163(2):277–296

Levy R, Nullo FE (1970a) Terebratulidos Devonicos de Argentina-1 Cranaena y Scaphiocoelia. Ameghiniana 7(3):264–274

Levy R, Nullo FE (1970b) Terebratulidos Devonicos de Argentina II Pleurothyrella. Ameghiniana 7(4):369–378

Loske WP (1992) Sedimentologie, Herkunft und geo tektonische Entwicklung paläozoischer Gesteine der Präkordillere West-Argentiniens. Münch Geol H 7:1–155 (Munchen)

Loske WP (1994) The West-Argentine Precordillera: a Paleozoic Back arc Basin.Z Dt. Geol Ges 145:379–391

Loske WP (1995) 1.1Ga old zircons in W Argentina: implications for sedimentary provenance in the Paleozoic of Western Gondwana: Neues Jahrbuch für Geologie und Paläontologie Monatshefte, pp 51–64

Ludwing KR (2001) Users manual for Isoplot/EX (Rev. 2.49): a geochronological toolkit for microsoft excel. Berkeley Geochronol Center Spec Publ 1:55

Mange MA, Maurer HF (1992) Heavy minerals in colour. Chapman and Hall, London, UK

Massonne HJ, Calderón M (2008) PT evolution of metapelites from the Guarguaraz Complex, Argentina: evidence for Devonian crustal thickening close to the western Gondwana margin. Rev Geol Chile 35:1–17

McDaniel DK, McLennan SM, Hanson GN (1997) Provenance of Amazon fan muds: constraints from Nd and Pb isotopes. In: Proceedings of the ocean drilling program. Scientiic results, vol 155, pp 169–176

McLennan SM (1989) Rare earth elements in sedimentary rocks: inluence of provenance and sedimentary processes. In: Lipin BR, McKay GA (eds) Geochemistry and mineralogy of rare earth elements. Reviews in Mineralogy, vol 21, pp 169–200

McLennan SM, Taylor S (1991) Sedimentary rocks and crustal evolution: tectonic setting and secular trends. J Geol 99:1–21

McLennan SM, Taylor SR, McCulloch MT, Maynard JB (1990) Geochemical and Nd-Sr isotopic composition of deep-sea turbidites. Geochim Cosmochim Acta 54:2015–2050

McLennan SM, Hemming S, McDaniel DK, Hanson GN (1993) Geochemical approaches to sedimentation, provenance and tectonics. In: Johnsson MJ, Basu A (eds) Processes controlling the composition of clastic sediments. Geological Society of America. Special paper, vol 285. pp 21–40

McLennan SM, Bock B, Hemming SR, Hurowitz JA, Lev SM, McDaniel DK (2003) The roles of provenance and sedimentary processes in the geochemistry of sedimentary. In: Lentz DR (ed) Geochemistry of sediments and sedimentary rocks: evolutionary considerations to mineral deposit-forming environments, vol 4. Geological Association of Canada, pp 7–38

Mingramm A (1985) Secciones estructurales de la Cuenca de Cuyo y extension palispastica. Escala 1:200000. 10 secciones, Buenos Aires (Unpublished)

Nance WB, Taylor SR (1976) Rare earth element patterns and crustal evolution—I. Australian Post-Archean sedimentary rocks. Geochim Cosmochim Acta 40:1539–1551

Nance WB, Taylor SR (1977) Rare earth element patterns and crustal evolution—II. Archean sedimentary rocks from Kalgoorlie Australia. Geochim Cosmochim Acta 41(2):225–231

Nesbitt HW, Young YM (1982) Early Proterozoic climates and plate motions inferred from major element chemistry of lutites. Nature 299:715–717

Nesbitt HW, Young GM (1984) Prediction of some weathering trends of plutonic and volcanic rocks based on thermodynamic and kinetic considerations. Geochim Cosmochim Acta 48:1523–1534

Nesbitt HW, Young GM (1989) Formation and diagenesis of weathering profiles. J Geol 97:129–147

Nesbitt HW, Young GM, McLennan SM, Keays RR (1996) Effects of chemical weathering and sorting on the petrogenesis of siliciclastic sediments, with implications for provenance studies. J Geol 104:525–542

Ortiz A, Zambrano JJ (1981) La provincia geológica Precordillera oriental: VIII Congreso Geológico Argentino, vol 3, pp 59–74

Padula E, Rolleri E, Mingramm AR, Criado Roque P, Flores M, Baldis BA (1967) Devonian of Argentina: International symposium on the Devonian system. Canadian society of petroleum geologists, Calgary, Canada, vol 2, pp 165–199

Peralta SH (1991) La comunidad de *Pleurothyrella* en la Formación Talacasto (Devónico inferior), Precordillera Central Sanjuanina, Argentina. Rev Yacimientos Pet Fisc Boliv 12:139–143

Peralta SH (2005a) The lower emsian?-Middle Devonian? Extensional basins of the Los Sombreros and Rinconada Formations: its tecto-sedimentary signiicance in the evolution of the Precordillera. Gondwana 12:289

Peralta SH (2005b) Formación Los Sombreros: un evento diastrófico extensional del Devónico (inferor?-medio?) en la Precordillera Argentina. XVI Congreso Geológico Argentino, vol 4, pp 322–326. La Plata

Peralta SH (2013) Devónico de la sierra de la Invernada, Precordillera de San Juan, Argentina: revisión estratigráfica e implicancias paleogeográfícas. Rev Asoc Geol Argent 70(2):202–215

Peralta SH, Aceñolaza FG (1988) *Paleo helminthoida ruchholz* (traza fósil) en los estratos basales de la Formación Punta Negra (Devónico medio- superior?), en el perfil del Río San Juan, Precordillera Central del Oeste Argentino. Correl Geol 5:195–198

Peralta SH, y Ruzycki de Behrenstein LJ (1990) Icnofacies asociadas a facies turbiditicas de la Formación Punta Negra (Devónico medio- superior?), en el perfil de los Caracoles, Precordillera Central sanjuanina, Argentina. Reun Argent Sediment III:334–338

Peralta SH, Chávez IJ, Cuadra IJ y Ortiz MJ (2008) Estratigrafía del Silúrico Devónico de la sierra de la Invernada Precordillera Central de San Juan: signiicado tecto-sedimentario. XVII Congreso Geológico Argentino. Actas tomo 1, pp 370–371. San Salvador de Jujuy, Argentina

Peralta SH, Pereyra ME, León LI, Villegas CR (2010) Olistostromas del Devónico en la Precordillera de San Juan: Significado estratigráico y tectosedimentario. Jornada de Ciencia y Técnica en la UNSJ 2010

Poiré D, Morel E (1996) Procesos sedimentarios vinculados a la depositación de niveles con plantas en secuencias Siluro-Devónicas de la Precordillera Argentina, vol VI. Reunión Argentina de Sedimentología, Actas, pp 205–210

Pupin JP (1980) Zircon and granitepetrology. Contrib Mineral Petrol 73:207–220

Racheboeuf PR, Herrera ZA (1994) On some new malvinokaffric Silurian and Devonian chonetacean brachiopods and reclassification of others. Neues Jahrbuch Geol Paläontol 9:541–560

Racheboeuf PR, Dalenz Farjat A, Lefebvre B (1998) The Devonian Gamoneda section of southern Bolivia: new biostratigraphical and palaeobiogeographical data. Rev Esp Paleontol 13:175–186

Ragona D, Anselmi G, González P y Vujovich G (1995) Mapa Geológico de la provincia de San Juan (República Argentina) a Escala 1:500.000. Servicio Geológico y Minero Argentino

Ramacciotti CD, Baldo EG, Casquet C (2015) U-Pb SHRIMP detrital zircon ages from the Neoproterozoic Difunta Correa Metasedimentary Sequence (Western Sierras Pampeanas, Argentina): Provenance and paleogeographic implications. Precambr Res 270:39–49

Ramos VA (1999) Rasgos estructurales del territorio argentino. Geol Argent 29(24):15–75

Ramos VA (2004) Cuyania, an exotic block to Gondwana: review of a historical success and the present problems. Gondwana Res 7(4):1009–1026

Ramos VA, Jordan TE, Allmendinger RW, Mpodozis C, Kay SM, Cortés JM, Palma M (1986) Paleozoic Terranes of the Central Argentine Chilean Andes. Tectonics 5:855–880

Ramos VA, Dallmeyer RD, Vujovich G (1998) Time constraints on the Early Palaeozoic docking of the Precordillera, central Argentina. Geol Soc Lond Spec Pub 142(1):143–158

Rapela CW, Coira B, Toselli A, Saavedra J (1992) The lower Paleozoic magmatism of southwestern Gondwana and the evolution of the Famatinian Orogen. Int Geol Rev 34(11):1081–1142

Rapela CW, Pankhurst RJ, Casquet C, Baldo E, Saavedra J, Galindo C (1998) Early evolution of the Proto-Andean margin of South America. Geology 26(8):707–710

Rapela CW, Pankhurst RJ, Casquet C, Baldo E, Galindo C, Fanning CM, Dahlquist JM (2010) The Western Sierras Pampeanas: protracted Grenville-age history (1330–1030 Ma) of intra-oceanic arcs, subduction–accretion at continental-edge and AMCG intraplate magmatism. J South Am Earth Sci 29(1):105–127

Rudnick RL, Gao S (2003) Composition of the continental crust. In: Rudnick RL (ed) The crust: Holland HD, Turekian KK (eds) Treatise on geochemistry, vol 3, Elsevier-Pergamon, Oxford, pp 1–64

Rustan JJ (2011) Los trilobites devonicos de Precordillera Argentina: sistematica, ilogenia, paleobiogeografia y bioestratigrafia. Tesis Doctoral. Universidad Nacional de Cordoba. Facultad de Ciencias Exactas, Fisicas y Naturales, 352 p (Unpublished)

Rustán JJ, Vaccari NE (2010) The Aulacopleurid trilobite Maurotarion-Alberti, 1969, in the Silurian-Devonian of Argentina: systematic, phylogenetic and paleobiogeographic significance. J Paleontol 84(6):1082–1098

Salas MJ, Rustán JJ, Starren AF (2013) Lower and Middle Devonian Malvinokaffricostracods from the Precordillera Basin of San Juan, Argentina. J South Am Earth Sci 45:56–68

Sánchez TM, Waisfeld B, Benedetto JL (1991) Lithofacies, taphonomy, and brachiopod assemblages in the Silurian of western Argentina. A review of Malvinokafric Realm communities. J South Am Earth Sci 4:307–329

Sato AM, Tickyj H, Llambías EJ, Basei MAS, González PD (2004) Las Matras Block, Central Argentina (37 S-67 W): the southernmost Cuyania terrane and its relationship with the Famatinian orogeny. Gondwana Res 7(4):1077–1087

Sato K, Basei MAS, Ferreira CM, Vlach SRF, Ivanuch W, Siga Jr O, Onoi AT (2010) In situ U-Th-Pb Isotopic Analyses by Excimer Laser Ablation/ICP-MS on Brazilian Xenotime Megacrystal: First U-Pb Results at CPGeo-IG-USP. VII SSAGI. CD Room, Brasilia

Sterren AF, Rustán JJ, Salas MJ (2015) First middle Devonian bivalves from Argentina, new records from the Punta Negra formation and insights on middle Paleozoic faunas from Precordillera Basin. Ameghiniana 52(3):334–349

Sun SS, McDonough WF (1989) Chemical and isotopic systematics of oceanic basalts: implications for mantle composition and processes. In: Saunders AD, Norry MJ (eds) Magmatism in the ocean basins. Geological Society Special Publication, vol 42, pp 313–345

Taylor HP, McLennan SM (1985) The continental crust: its composition and evolution. Blackwell, Oxford

Thomas WA, Astini RA (2003) Ordovician accretion of the Argentine Precordillera terrane to Gondwana: a review. J South Am Earth Sci 16(1):67–79

Tickyj H, Tomezzoli RN, Basei MA, Fernandez MA, Blatter JM, Rodriguez N, Gallo LC (2015) Geología de la Formación Piedras de Ailar, basamento granitico del Distrito Minero Agua Escondida, Mendoza. III Simposio Petrología y Metalogénesis Asociada, Abstract, p 2. General Roca, Río Negro Argentina

Varela R, Basei MA, González PD, Sato AM, Naipauer M, Neto MC, Meira VT (2011) Accretion of Grenvillian terranes to the southwestern border of the Río de la Plata craton, western Argentina. Int J Earth Sci 100(2–3):243–272

Vieira de Luca PH, Basilici G (2008) Análogos de reservatórios de rampa de água profunda: sistemas ricos em lama (unidade de Apiúna-SC) e emareia (Formação Punta Negra, Pré-Cordilheira Argentina). Braz J Geol 38(1):140–158

Vieira de Luca PH, Basilici G (2013) A prodeltaic system controlled by hyperpycnal flows and storm waves: reinterpretation of the Punta Negra Formation (Lower-Middle Devonian, Argentine Precordillera). Braz J Geol 43(4):673–694

Vujovich GI, Porcher C, Chernicoff CJ, Fernandes LA, Pérez DJ (2005) Extremo norte del basamento del terreno Cuyania: nuevos aportes multidisciplinarios para su identificación. Asoc Geol Argent Serie D, Publ Espec 8:15–41

Willner AP, Gerdes A, Massonne HJ, Schmidt A, Sudo M, Thomson SN, Vujovich G (2011) The geodynamics of collision of a microplate (Chilenia) in Devonian times deduced by the pressure–temperature–time evolution within part of a collisional belt (Guarguaraz Complex, W-Argentina). Contrib Miner Petrol 162(2):303–327